Marine Micropaleontology 88–89 (2012) 15–35

Contents lists available at SciVerse ScienceDirect

Marine Micropaleontology

journal homepage: www.elsevier.com/locate/marmicro

Multiple early Eocene benthic foraminiferal assemblage and $\delta^{13}C$ fluctuations at DSDP Site 401 (Bay of Biscay — NE Atlantic)

Simon D'haenens [a,*], André Bornemann [b], Peter Stassen [a], Robert P. Speijer [a]

[a] Department of Earth and Environmental Sciences, KU Leuven, Celestijnenlaan 200E, B-3001 Leuven, Belgium
[b] Institut für Geophysik und Geologie, Universität Leipzig, Talstrasse 35, D-04103 Leipzig, Germany

ARTICLE INFO

Article history:
Received 11 May 2011
Received in revised form 17 February 2012
Accepted 20 February 2012

Keywords:
Eocene
Benthic foraminifera
Ecology
Hyperthermal
Deep Sea Drilling Project

ABSTRACT

Within the last decade, several early Eocene hyperthermals have been detected globally. These transient warming events have mainly been characterized geochemically – using stable isotopes, carbonate content measurements or XRF core scanning – yet detailed micropaleontological records are sparse, limiting our understanding of the driving forces behind hyperthermals and of the contemporaneous paleoceanography. Here, detailed geochemical and quantitative benthic foraminiferal records are presented from lower Eocene pelagic sediments of Deep Sea Drilling Project Site 401 (Bay of Biscay, northeast Atlantic). In calcareous nannofossil zone NP11, several clay-enriched levels correspond to negative $\delta^{13}C$ and $\delta^{18}O$ bulk-rock excursions with amplitudes of up to ~0.75‰, suggesting that significant injections of ^{12}C-enriched greenhouse gasses and small temperature rises took place. Coeval with several of these hyperthermal events, the benthic foraminiferal record reveals increased relative abundances of oligotrophic taxa (e.g. *Nuttallides umbonifera*) and a reduction in the abundance of buliminid species followed by an increase of opportunistic taxa (e.g. *Globocassidulina subglobosa* and *Gyroidinoides* spp.). These short-lived faunal perturbations are thought to be caused by reduced seasonality of productivity resulting in a decreased C_{org} flux to the seafloor. Moreover, the sedimentological record suggests that an enhanced influx of terrigenous material occurred during these events. Additionally, the most intense $\delta^{13}C$ decline (here called level δ) gives rise to a small, yet pronounced long-term shift in the benthic foraminiferal composition at this site, possibly due to the reappraisal of upwelling and the intensification of bottom water currents. These observations imply that environmental changes during (smaller) hyperthermal events are also reflected in the composition of deep-sea benthic communities on both short (<100 kyr) and longer time scales. We conclude that the faunal patterns of the hyperthermals observed at Site 401 strongly resemble those observed in other deep-sea early Paleogene hyperthermal deposits, suggesting that similar processes have driven them.

1. Introduction

The Paleocene–Eocene Thermal Maximum (PETM; ~55.8 Ma) is a geologically brief (~170 kyr; Röhl et al., 2007) climate perturbation that is characterized by an increase of global temperatures by ~5–10 °C (Kennett and Stott, 1991; Zachos et al., 2003; Tripati and Elderfield, 2005; Sluijs et al., 2008). The onset of the PETM is also marked by a prominent negative carbon isotope excursion (CIE) of more than 2‰ in both marine and terrestrial sedimentary sequences (McInerney and Wing, 2011) and by $CaCO_3$ dissolution in deep-sea sediments (Zachos et al., 2005; Zeebe and Zachos, 2007). The CIE and dissolution phenomena associated with this hyperthermal event are generally considered to be caused by a massive injection of ^{12}C-rich carbon released by methane hydrates into the ocean–atmosphere system, yet the sources and mass of the input remains uncertain and controversial (Dickens, 2011). The repercussions on faunal and floral communities were significant, with numerous biotic turnovers both on land and in the oceans (Crouch et al., 2001; Bralower, 2002; Raffi et al., 2005, 2009; Wing et al., 2005; Gibbs et al., 2006; Gingerich, 2006; Scheibner and Speijer, 2008), but the most notable biotic event is the large extinction (30%–50% of species) of deep-sea benthic foraminifera (Thomas, 1990, 1998, 2003, 2007; Kennett and Stott, 1991; Thomas and Shackleton, 1996). This extinction sharply contrasts to the K–Pg boundary, when deep-sea benthic foraminiferal assemblages displayed no significant changes (Culver, 2003; Alegret and Thomas, 2007, 2009).

Thomas and Zachos (2000) suggested that the PETM might not be a singular event, but only the most extreme example of a series of similar events. The first evidence for this hypothesis was a stacked high-resolution global carbon isotope record based on early Paleogene deep-sea sites (DSDP Sites 550 and 577; ODP Sites 690 and 1051), which revealed several late Paleocene and early Eocene CIEs, and which were labeled with an alphanumeric scheme (A–K) (Cramer et al., 2003). Several studies have confirmed the

* Corresponding author. Tel.: +32 16 32 64 29; fax: +32 16 32 29 80.
E-mail address: simon.dhaenens@ees.kuleuven.be (S. D'haenens).

0377-8398/$ – see front matter © 2012 Elsevier B.V. All rights reserved.
doi:10.1016/j.marmicro.2012.02.006

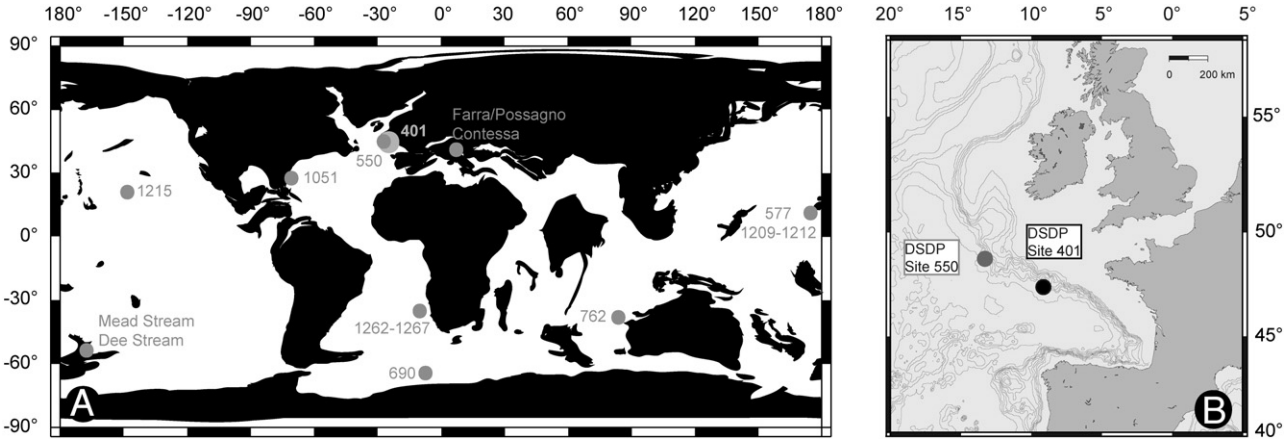

Fig. 1. Location of DSDP Site 401. (A) Paleogeographic reconstruction (~53 Ma; http://www.odsn.de/odsn/services/paleomap/paleomap.html) with locations of DSDP Sites 401, 550, 577 and ODP Sites 690, 762, 1051, 1209–1212, 1215, 1262–1267 and land sections (Italy: Farra, Possagno, Contessa; New Zealand: Mead Stream, Dee Stream). (B) Present-day bathymetric map with locations of DSDP Sites 401 and 550.

hyperthermal nature of some of these CIEs, among those H1 (also ETM-2; ~53.7 Ma; Lourens et al., 2005; Nicolo et al., 2007; Galeotti et al., 2010), H2 (~53.6 Ma; Stap et al., 2009, 2010a,b), I1 and I2 (~53.20 and ~53.18 Ma, respectively; Nicolo et al., 2007; Leon-Rodriguez and Dickens, 2010) and K (also ETM-3 or X-event; ~52.5 Ma; Agnini et al., 2009; Galeotti et al., 2010). Furthermore, it appears that these events all share a similar origin, which is based on their diagnostic frequencies due to orbital forcing (Lourens et al., 2005; Nicolo et al., 2007; Westerhold et al., 2007; Galeotti et al., 2010; Sexton et al., 2011), although the PETM seems to be out of phase with the long-term eccentricity cycle of ~400 kyr (Zachos et al., 2010).

Nevertheless, our present understanding of these post-PETM hyperthermals remains relatively unconstrained as little is known about the biotic responses and the supposed paleoceanographic changes. Moreover, if hyperthermals were a recurrent aspect of the early Paleogene greenhouse world, systematic faunal responses would be expected. Therefore, a high-resolution investigation of faunal and isotope patterns across PETM-like events in the early Eocene may provide more detailed information on the possible

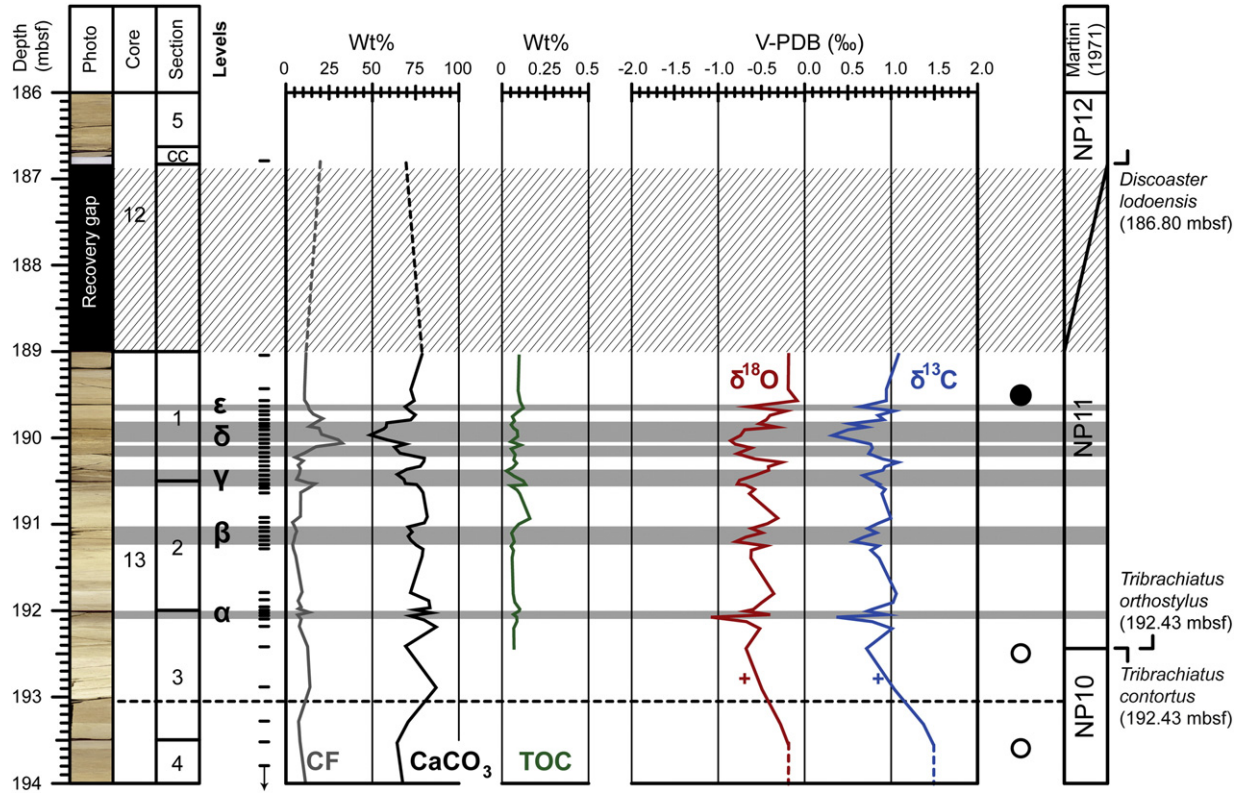

Fig. 2. Core photograph, stratigraphy and geochemical data plotted versus depth. Coarse fraction (CF), $CaCO_3$ content, total organic carbon (TOC) content and stable isotope bulk records of cores 13 and 12 are shown next to the nannoplankton biozonation (Martini, 1971). Dots represent low-resolution magnetostratigraphic data by Hailwood (1979) (Black dot = normal polarity; white dot = reversed polarity). Tick marks next to the core photograph represent all samples. The dashed line at 193.00 mbsf represents a lithological break. Hatched interval represents the recovery gap at the base of core 12. Crosses represent bulk stable isotope data from Létolle et al. (1979).

linkage between global warming events, paleoceanography and the sensitivity of deep-sea biota.

To address these issues, we focused on lower Eocene sediments of Deep Sea Drilling Project (DSDP) Site 401 (Bay of Biscay, northeast Atlantic), one of the most northern deep-sea drilling sites to provide Eocene pelagic carbonates. While previous geochemical and micropaleontological studies of Site 401 focused on the interval bracketing the PETM (Pak and Miller, 1992; Pardo et al., 1997; Nunes and Norris, 2006), this study aims at investigating the postulated faunal responses of post-PETM hyperthermal events. The studied sequence provides an excellent opportunity to detect and characterize hyperthermals in the deep-sea realm of the northeast Atlantic. By generating a detailed quantitative foraminiferal record complemented by stable isotopes, we attempt to assess the sensitivity of early Eocene benthic communities with respect to oceanographic properties such as C_{org} flux to the sea floor, ocean circulation, stratification, acidification and warming.

2. Material and methods

2.1. DSDP Site 401

Deep Sea Drilling Project (DSDP) Site 401 (47°25.65′ N, 08° 48.62′ W; 2495 m present water depth) is located on Meriadzek Terrace, a tilted fault block on the northern margin of the Bay of Biscay, northeast Atlantic Ocean (Montadert et al., 1979a; Fig. 1). In the early Paleogene, this site was located at a latitude of ~43°N (McInerney and Wing, 2011). In total, 50 samples have been studied from the sedimentary succession consisting of lower Eocene pale grayish-brown, calcareous nannofossil chalks of cores 12 and 13 (Fig. 2 and Table 1). From core 13, an interval of 5.8 m (194.80–189.00 mbsf) was sampled in relatively low resolution (~10–40 cm) in the lowermost and uppermost part of the core and in high resolution (~4–5 cm) across several marly levels present in this interval. From core 12 only the core catcher was sampled.

Table 1
Geochemical and lithological data used in this study. $CaCO_3$ content, coarse fraction (CF; >63 μm), total organic carbon (TOC) and stable isotopes. 'X' marks the samples used for the quantitative micropaleontological analysis.

Core	Section	Top (cm)	Bottom (cm)	Depth (mbsf)	$CaCO_3$ (wt.%)	CF (% >63 μm)	TOC (wt.%)	$\delta^{13}C$ (‰ V-PDB)	$\delta^{18}O$	Fauna
12	CC	6	8	186.80	69.35	20.53	–	–	–	X
13	1	5	8	189.05	79.06	12.41	0.11	1.10	−0.17	X
13	1	45	47	189.45	72.49	11.60	0.10	0.96	−0.17	X
13	1	58	59	189.58	74.48	11.50	0.11	0.96	−0.07	X
13	1	65	66	189.65	69.18	13.53	0.13	0.66	−0.64	X
13	1	70	71	189.70	71.71	14.28	0.10	1.05	−0.20	X
13	1	75	76	189.75	75.15	16.57	0.07	0.87	−0.39	X
13	1	80	81	189.80	72.49	22.06	0.08	0.93	−0.43	X
13	1	84.5	85.5	189.85	58.57	17.57	0.06	0.54	−0.51	X
13	1	88.5	90	189.89	58.17	14.34	0.07	0.73	−0.31	X
13	1	91.5	92.5	189.92	56.78	19.92	0.10	0.52	−0.68	X
13	1	98	99	189.98	48.92	21.39	0.10	0.34	−0.73	X
13	1	104	105	190.04	59.14	30.94	0.06	0.61	−0.84	X
13	1	108	109	190.08	69.49	33.39	0.12	0.78	−0.79	X
13	1	112.5	113.5	190.13	63.06	18.07	0.06	0.80	−0.60	X
13	1	119	120	190.19	66.21	11.65	0.08	0.76	−0.77	X
13	1	125	126	190.25	80.35	6.10	0.08	0.92	−0.56	X
13	1	129	132.5	190.29	80.10	10.74	0.09	1.10	−0.25	–
13	1	134	135	190.34	78.00	7.89	0.07	0.95	−0.40	X
13	1	138	139	190.38	70.14	9.12	0.03	0.92	−0.40	X
13	1	144	145	190.44	64.64	8.51	0.08	0.69	−0.57	X
13	1	149.5	150.5	190.50	68.57	6.93	0.13	0.79	−0.74	X
13	2	4	5.5	190.54	69.35	13.62	0.15	0.88	−0.76	X
13	2	5	6.5	190.55	75.85	17.65	0.06	0.86	−0.67	X
13	2	10	11	190.60	78.02	13.85	0.09	0.95	−0.56	X
13	2	14.5	15.5	190.65	79.57	9.31	0.11	0.91	−0.62	X
13	2	43	46	190.93	82.09	9.22	0.17	1.01	−0.30	X
13	2	49.5	50.5	191.00	80.35	4.61	0.10	0.86	−0.42	X
13	2	55	56	191.05	70.92	5.86	0.08	0.74	−0.60	X
13	2	60	61	191.10	73.28	7.00	0.06	0.85	−0.48	X
13	2	65	66	191.15	70.95	6.02	0.07	0.70	−0.67	X
13	2	70	71	191.20	72.49	5.48	0.08	0.58	−0.78	X
13	2	75	76	191.25	75.64	4.63	0.06	0.87	−0.43	X
13	2	80	81	191.30	79.57	5.07	0.07	0.78	−0.60	X
13	2	88.5	91	191.39	79.06	6.44	0.07	0.88	−0.61	–
13	2	130	131.5	191.80	72.32	10.12	0.07	1.08	−0.34	X
13	2	140	142	191.90	82.93	7.79	0.08	1.04	−0.48	X
13	2	148	150	191.98	83.63	9.61	0.11	0.79	−0.58	X
13	3	0	2	192.00	75.15	8.05	0.11	0.74	−0.67	X
13	3	4	7	192.04	84.34	14.17	0.07	0.96	−0.38	X
13	3	7	8	192.07	72.32	7.52	0.09	0.38	−1.07	X
13	3	12	14	192.12	80.10	9.61	0.09	0.80	−0.66	X
13	3	20	22	192.20	87.17	8.49	0.07	1.03	−0.50	X
13	3	43	45	192.43	69.49	13.27	0.08	0.73	−0.66	X
13	3	90	92	192.90	87.17	14.70	–	1.06	−0.48	X
13	3	130	131.5	193.30	70.90	8.08	–	1.39	−0.26	X
13	4	3	5	193.53	64.54	8.93	–	1.50	−0.18	X
13	4	43	44.5	193.93	68.07	11.37	–	–	–	–
13	4	93	95	194.43	68.78	17.69	–	–	–	–
13	4	130	132	194.80	64.54	5.52	–	1.50	−0.18	X

2.2. Stratigraphy

Stratigraphic control was obtained using a biostratigraphic zonation scheme based on calcareous nannofossils. Our results are well in line with those of Müller (1979). We place the NP10/NP11 boundary at 192.43 mbsf, where the highest occurrence (HO) of *Tribrachiatus contortus* and a crossover in abundance of *T. contortus* and *T. orthostylus* occurs, following Martini (1971) and as amended by Raffi et al. (2005). Due to the partial core recovery of core 12 (~75%), the actual NP11/NP12 boundary (lowest occurrence (LO) of *Discoaster lodoensis*) could not be unequivocally identified and is therefore located between 189.05 mbsf and 186.80 mbsf. Low-resolution magnetochronostratigraphic data (Fig. 2) are taken from Hailwood (1979). Basically, the studied interval includes the top of Biozone NP10 and the (partially) recovered biozone NP11.

2.3. Geochemistry and stable isotopes ($\delta^{13}C$, $\delta^{18}O$)

$CaCO_3$ content, total organic carbon (TOC) content and stable isotope values of the bulk sediment of all samples are given in Table 1.

Samples were analyzed with respect to their $CaCO_3$ content employing the carbonate bomb technique (Müller and Gastner, 1971). In addition, the total organic carbon (TOC) content was measured using an ELTRA Metaly CS 100/100 at the Universität Leipzig. For the TOC measurements approximately 100 mg of sediment were decalcified with 10% HCL and dried for about 12 h at 90 °C. The precision for replicate analyses is about 2 wt.% for $CaCO_3$ and 0.05 wt.% for TOC.

Stable isotope compositions of the bulk sediments were measured using a Kiel III online carbonate preparation line connected to a ThermoFinnigan 252 mass spectrometer at the Universität Erlangen, Germany. The crushed and dried bulk material reacted with 100% phosphoric acid (density > 1.9, Wachter and Hayes, 1985) at 75 °C. All values are reported in per mil relative to Vienna Pee Dee Belemnite (V-PDB) by assigning a $\delta^{13}C$ value of +1.95‰ and a $\delta^{18}O$ value of −2.20‰ to NBS19. Reproducibility was checked by replicate analyses of laboratory standards (IAEA-CO1) and is better than ±0.02 (1σ) for both $\delta^{13}C$ and $\delta^{18}O$.

2.4. Fauna

For the faunal study, 46 out of the initial 50 samples were analyzed due to lack of sufficient material in the remaining four samples. The samples were dried at ~50 °C, weighed, soaked in tap water for 24 h, gently washed under running water through a 63 μm sieve, dried and weighed again. Benthic and planktic foraminifera were counted from a representative split (using an ASC micro-splitter), so that the number of benthic and planktic foraminifera per gram of sediment (BFN and PFN, respectively) could be calculated. From the same split, the percentage of planktic foraminifera (%P) was calculated (~425–1700 specimens/split; average of ~900). %P can only be applied to determine depth of neritic to upper bathyal settings (> 30–1200 m depth) in (sub-) recent settings with some certainty (van der Zwaan et al., 1990) and we primarily used %P to assess possible dissolution intervals since planktic foraminifera are more prone to dissolution than benthic foraminifera (van der Zwaan et al., 1990; Nguyen et al., 2009). Concerning depth estimates, we followed the bathymetric division defined in Van Morkhoven et al. (1986): upper bathyal = 200–600 m, middle bathyal = 600–1000 m, lower bathyal = 1000–2000 m and abyssal > 2000 m.

The quantitative foraminiferal study was performed on representative aliquots. All benthic foraminifers were picked from the > 63 μm residues and were mounted on reference slides. The size fraction > 63 μm was considered as most appropriate for this study, as it enabled us to investigate small opportunistic taxa and slender (serial) forms that may occur in deep-sea environments (Schröder et al., 1987). Furthermore, as has been shown for the PETM, during stressed marine conditions, small species and small specimens generally predominate (Thomas, 1998; Kaiho et al., 2006; Alegret et al., 2010). Per sample, 212 to 978 specimens were picked (average of ~383). Up to four percent of the picked tests ended up being unidentified because of preservation problems such as fragmentation and calcite overgrowth so that characteristic features could not be determined, or because of indistinct juvenile forms.

Taxonomic assignments were based on and adapted from Proto Decima and Bolli (1978), Schnitker (1979), Schnitker and Tjalsma (1980), Boltovskoy (1983), Miller (1983), Tjalsma (1983), Tjalsma and Lohmann (1983), Clark and Wright (1984), Miller et al. (1985), Thomas (1985), Van Morkhoven et al. (1986), Hulsbos (1987), Miller and Katz (1987), Boltovskoy and Boltovskoy (1989), Thomas (1990), Müller-Merz and Oberhänsli (1991), Nomura (1991), Boltovskoy et al. (1992), Mackensen and Berggren (1992), Boltovskoy and Watanabe (1993), Boltovskoy and Watanabe (1994), Nomura (1995), Alegret and Thomas (2001), Holbourn and Henderson (2002), Katz et al. (2003), Nomura and Takata (2005), Sztrákos (2005), Ernst et al. (2006), Ortiz and Thomas (2006), Alegret and Thomas (2007) and Alegret et al. (2009). The generic classification of Loeblich and Tappan (1988) was used and adapted in some instances. The most important taxa were photographed using Scanning Electron Microscopy (SEM) and their preservation

Plate 1. SEM micrographs of unsonicated specimens. All specimens are shown at the same scale (scale bar = 100 μm), unless indicated otherwise.

1. *Nuttallides truempyi* (Nuttall). 189.92 mbsf, 1a) umbilical view, 1b) spiral view.
2. *Oridorsalis umbonatus* (Reuss). 191.20 mbsf, 2a) umbilical view, 2b) spiral view.
3. *Nonion havanense* Cushman and Bermúdez. 191.25 mbsf.
4–6. *Bolivina huneri/crenulata* 4) *Bolivina huneri* Howe. 194.80 mbsf. 5) *Bolivina huneri/Bolivinoides crenulata* intermediate. 190.34 mbsf. 6) *Bolivinoides crenulata* (Cushman). 194.80 mbsf.
7. *Anomalinoides praespissiformis* (Cushman and Bermúdez). 194.80 mbsf. 7a) umbilical view, 7b) apertural view, 7c) spiral view.
8. *Bulimina tuxpamensis* Cole. 194.80 mbsf.
9. *Aragonia aragonensis* (Nuttall). 193.53 mbsf.
10. *Tappanina selmensis* (Cushman). 194.80 mbsf.
11. *Bulimina thanetensis* Cushman and Parker. 194.80 mbsf.
12–13. *Bulimina virginiana* (Cushman). 194.80 mbsf.
14. *Praebulimina reussi* (Morrow). 194.80 mbsf.
15. *Praebulimina* sp.1. 194.80 mbsf.
16. *Eponides bollii* (Cushman and Renz). 194.80 mbsf.
17. *Siphonina tenuicarinata* Cushman. 194.80 mbsf.
18. *Anomalinoides alazanensis* (Nuttall). 194.80 mbsf. 18a), spiral view, 18b) apertural view, 18c) umbilical view.
19. *Seabrookia lagenoides* Ten Dam. 189.89 mbsf.
20. *Pseudoparrella minuta* Olsson. 194.80 mbsf. 20a) umbilical view, 20b), spiral view.
21. *Cibicidoides eocaenus* (Gümbel). 194.80 mbsf. 21a) umbilical view, 21b) apertural view, 21c) spiral view.
22–23. *Angulogerina muralis* (Terquem). 22) 189.92 mbsf, 23) 186.80 mbsf.
24. *Brizalina carinata* (Terquem). 189.70 mbsf.
25. *Pleurostomella paleocenica* Cushman. 193.53 mbsf.

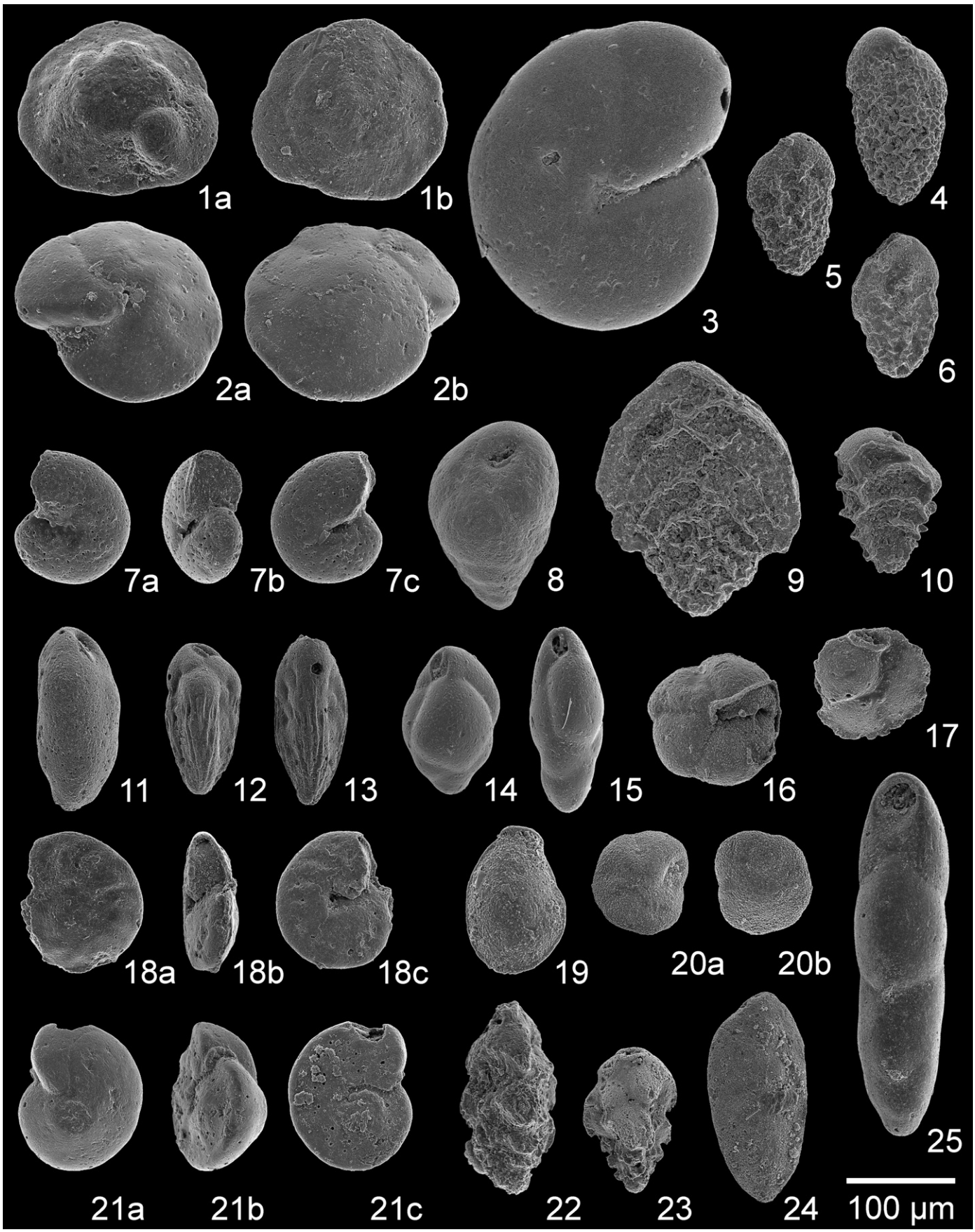
1a
1b
3
4
5
2a
2b
6
7a
7b
7c
8
9
10
11
12
13
14
15
16
17
18a
18b
18c
19
20a
20b
25
21a
21b
21c
22
23
24
100 µm

was evaluated (See Plates 1 and 2). All original species descriptions were checked with the online version of the Ellis and Messina catalog (http://www.micropress.org).

The qualitative parameters used to characterize the benthic assemblages were the following:

Shannon–Wiener index	H′	$H' = -\Sigma p_i \ ln \ p_i$
Dominance (1-Simpson index)	λ	$\lambda = \Sigma(p_i^2)$

with n being the total number of individuals and p ($= n_i/\Sigma n$) the proportion of taxon (i). The percentage of endobenthic morphotypes (%endobenthics) was calculated using the probable microhabitat preferences inferred from benthic foraminiferal morphotype analysis (e.g. Corliss and Chen, 1988). Because this measure is rather problematic (e.g. Buzas et al., 1993), environmental parameters (e.g. trophic and oxic regime) were instead inferred from species with well-established paleoecological preferences (e.g. Table 3).

For the statistical analysis, we used the relative abundances of all samples and the PAST software package (Hammer et al., 2001; Hammer and Harper, 2006). A hierarchical cluster analysis (CA) using the Pearson correlation as the similarity coefficient was carried out. Both an R-mode (foraminiferal species) and a Q-mode analysis (samples) was performed on selected taxa occurring at a relative abundance of >2% in at least one sample. This cut-off value was chosen to improve reliability and relevance of the statistical analysis and to minimize downhole contamination effects. Despite the high number of species, we did not sort species into groups of taxonomically or morphologically related taxa because it was clear early on that several species from the same group did not display similar distribution patterns. Ultimately, a total of thirty-seven taxa were used for the CA. The same data set was used for a Detrended Correspondence Analysis (DCA). This method was used to distil the main benthic foraminiferal patterns and to compare these with various environmental variables. Where possible, both methods were used to determine the ecology of poorly-known benthic species based on their statistical relationship with (ecologically) better-known species.

Planktic foraminiferal test size was investigated for 17 samples from the 189.05–190.34 mbsf interval. Instead of measuring the size of individual specimens, the number of planktic foraminifera contained in separate size fractions was counted. Representative splits were sieved in four size fractions (63–125, 125–180, 180–250 and >250 μm). On average, ~1040 specimens were counted per sample (1σ: 240). Fragmented tests were excluded from these counts.

3. Results

3.1. Lithology and stable isotopes

$CaCO_3$ contents (Fig. 2) vary between 87.9% and 48.9% (average 72.5%), and closely correspond to sediment color: the highest values (~75–85%) appear in the pale nannofossil chalks, while lower $CaCO_3$ contents (~75–49%) are measured in four darker, marly levels. These moderately bioturbated reddish-colored levels, appear at the following intervals: 192.12–192.04 mbsf, 191.25–191.05 mbsf, 190.54–190.38 mbsf and at 190.19–189.85 mbsf, which we call α, β, γ and δ respectively (Fig. 2). It appears that these marly levels occur in a cyclic pattern, with each consecutive marly level displaying lower $CaCO_3$ percentages than the previous one. Overall, the highest $CaCO_3$ content occurs at the base of Biozone NP11 (~85%) while maximum values at the top of core 13 reach ~75%.

The amount of coarse fraction (>63 μm; Fig. 2) is relatively stable across the studied section and is on average 11.9% (by weight). However, values increase somewhat at the base of level γ (17.6%) and increase substantially within level δ: a maximum of 33.4% is reached at 190.08 mbsf, followed by a drop to 14.3% at 189.89 mbsf and a second peak of 22.1% at 189.80 mbsf. The amount of course fraction nearly doubles above level δ compared to below level δ. TOC values are extremely low, varying between 0.05 and 0.15% (average ~0.10%) and express no clear pattern.

The bulk $\delta^{13}C$ values vary between 0.34‰ and 1.50‰ and more specifically for biozone NP11 between 0.34‰ and 1.10‰ (Fig. 2). The $\delta^{13}C$ curve displays a similar pattern as the $CaCO_3$ content: heavier values in the pale, carbonate-rich intervals and lighter values in the marly levels. However, there seems to be another smaller negative excursion at ~189.65 mbsf, which we call ε, resulting in a total of five CIEs (α, β, γ, δ and ε). The maximum drop towards lighter values is 0.65‰, 0.29‰, 0.26‰, 0.76‰ and 0.39‰ for levels α, β, γ, δ and ε, respectively (Fig. 2). The small CIE at 190.19 mbsf is included in level δ as there is no return to background values, resulting in a stepwise appearance of the CIE of level δ. Similarly, the bulk carbonate $\delta^{18}O$ record displays a near-identical trend and the same five short negative excursions. The maximum drop towards lighter values is 0.57‰, 0.35‰, 0.20‰, 0.59‰ and 0.44‰ for levels α, β, γ, δ and ε, respectively (Fig. 2). Note that the CIEs of levels α and ε are produced by a single measurement and may represent outliers.

3.2. Foraminifera

In total, 118 benthic foraminiferal species and 72 genera were observed throughout the studied interval. The observed species composition is typical for early Eocene deep-sea benthic foraminiferal assemblages although some larger-sized species such as *Anomalinoides semicribrata*, *Cibicidoides laurisae*, *Pullenia* spp., *Quadrimorphina profunda*, *Abyssamina poagi*, *A. quadrata* and *Clinapertina inflata* – which are frequently reported for the early Eocene in classic taxonomic studies (e.g., Tjalsma and Lohmann, 1983) – were only rarely found at Site 401, most likely as a result of the small size fraction studied. Agglutinated taxa are scarce and consist of *Eggerella* sp., *Karrierella* sp., *Spiroplectammina spectabilis* and *Vulvulina mexicana*. The highest

Plate 2. SEM micrographs of unsonicated specimens. All specimens are shown at the same scale (scale bar = 100 μm), unless indicated otherwise.

1–2. *Cibicidoides ungerianus* (d'Orbigny). 1) 189.80 mbsf; 2) 189.92 mbsf, 2a) apertural view, 2b) spiral side
3. *Osangularia mexicana* (Cole). 189.92 mbsf.
4–5. *Globocassidulina subglobosa* (Brady). 4) 192.04 mbsf; 5) 194.80 mbsf.
6–7. *Gyroidinoides complanata* (Cushman and Stainforth). 194.80 mbsf. 6a) umbilical view, 6b) apertural view, 6c) spiral view, 7a) umbilical view, 7b) spiral view, 7c) detail of microboring ?*Ichnofossus* sp. (Nielsen et al., 2003) (scale bar = 10 μm).
8. *Buliminella grata* Parker and Bermúdez. 186.80 mbsf.
9. *Quadratobuliminella pyramidalis* de Klasz. 189.92 mbsf.
10. *Dentalina* sp.1. 189.85 mbsf (scale bar = 500 μm).
11. *Eggerella* sp.1. 189.92 mbsf.
12. *Bulimina semicostata* Nuttall. 190.65 mbsf.
13–14. *Nuttallides umbonifera* (Cushman). 194.80 mbsf. 13a) umbilical view, 13b) apertural view, 13c) spiral view, 14a, umbilical view, 14b, spiral view.
15. *Heronallenia pusilla* (Parr). 194.80 mbsf. 15a) spiral view, 15b) apertural view, 15c) umbilical view.
16. *Coryphostoma* sp.1. 189.70 mbsf.
17. *Turrilina brevispira* Ten Dam. 191.25 mbsf.
18. *Stilostomella gracillima* (Cushman and Jarvis). 186.80 mbsf.
19–20. *Stilostomella plummerae* (Cushman). 19) 189.70 mbsf, 20) 189.92 mbsf.

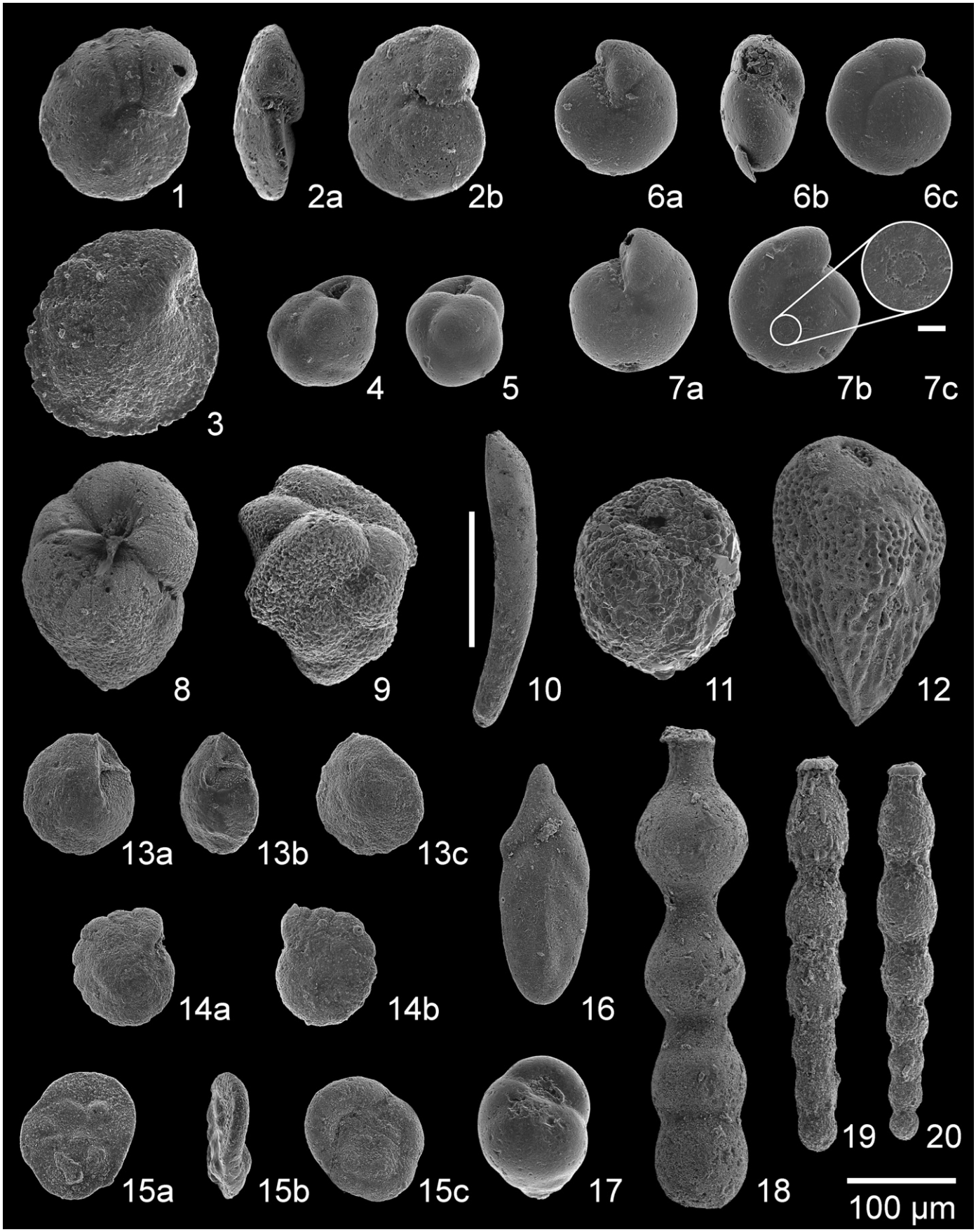
1
2a
2b
6a
6b
6c
3
4
5
7a
7b
7c
8
9
10
11
12
13a
13b
13c
14a
14b
16
15a
15b
15c
17
18
19
20
100 µm

abundances of these calcareous agglutinated taxa (~1%) are recorded in the marly levels.

The fauna is highly diverse, and the distribution of the relative abundances of the species is typical for deep-sea assemblages: few species occur with relative abundances of >5% while many rare species occur in relative abundances of <2%. The Shannon–Wiener index H′ (Fig. 3) ranges between 2.80 and 3.52, which reflects the relatively high diversity at this location, while dominance values (λ) range between 4 and 12%. The lowest H′ and highest λvalues are encountered in the samples at 189.98 (level δ), 189.05 and 186.80 mbsf.

The assemblages dominated by calcareous foraminifera indicate deposition above the CCD throughout and consist of mixed endo- and epibenthic morphogroups. In general, the %endobenthics (Fig. 3) is mostly close to 50% (37% to 62%) throughout the studied section. The %endobenthics shows a somewhat decreasing trend towards the top of the studied interval. The percentage of species of the Superfamily Buliminacea (*Aragonia*, *Bolivina*, *Brizalina*, *Bulimina*, *Buliminella*, *Coryphostoma*, *Fursenkoina*, *Praebulimina*, *Quadratobuliminella*, *Reussella*, *Siphogenerinoides*, and *Tappanina*) averages ~30% and also shows a slightly decreasing upward trend. Maximum values of up to 40% are reached below 193.00 mbsf and below level δ, and minimal values are reached in levels α (26%), δ (24%) and ε (22%). The large drop of Buliminaceae in levels δ and ε is associated with an increase in abundance of taxa with endobenthic morphotypes such as *Globocassidulina subglobosa*, *Stilostomella* spp. and *Dentalina* spp., stabilizing %endobenthics.

The %P (Fig. 3) throughout the interval is high, ranging from 95.25% to 99.05% (average of 97.25%; σ 0.84%). Although the observed changes in %P are rather small, in the order of a few percent, these variations could reveal significant changes in the ratio between the numbers of planktic and benthic foraminifera. Marly levels α and β show a slight drop in %P in concert with the $CaCO_3$ content, which could potentially be a sign of dissolution (van der Zwaan et al., 1990; Nguyen et al., 2009). In contrast, the three uppermost levels γ, δ and ε show maximal %P values of 97.55%, 99.05% and 97.95%, respectively.

Overall, the planktic foraminiferal numbers (PFN; Fig. 3) are very high, ranging between 3.0×10^4 and 3.0×10^5 per gram of sediment. The lowest values occur in level β and below the lithological break at 193.00 mbsf. Samples below this lithological break, which probably represents a hiatus, are more clayey than those above (Fig. 2) and show lower PFN values of ~3.0×10^4 per gram of sediment, in contrast with the samples above which reach values of up to 10 times higher. This difference is possibly caused by higher sedimentation rates and resulting dilution below the lithological break. Other high PFN values are found in level γ (1.4×10^5), above level δ (1.8×10^5) and near the top of core 13 (1.9×10^5). More or less the same pattern emerges for the benthic foraminiferal numbers (BFN; Fig. 3). These range between 800 and 1.3×10^4 per gram of sediment. Below the lithological break, values are close to 2.0×10^3, whereas above it they reach peak values of 1.3×10^4. Lowest values are encountered in level β (~800) and δ (~840). In contrast with the pattern of the PFN which is only slightly variable across levels δ and ε, the BFN display sudden four-fold drops in values reflecting the maximum %P of these particular levels.

3.2.1. Definition of faunal clusters based on cluster analysis

The relative abundances of the most common species are given in Fig. 4. Using the results of the R-mode CA, three large benthic foraminiferal clusters can be defined, grouping taxa that display similar distribution patterns through time.

- Cluster A (*N. umbonifera–G. subglobosa*): Defined by taxa that display large increases in relative abundance within the marly levels, and in particular level β, δ and ε. Common taxa include *Nuttallides umbonifera*, *G. subglobosa*, *Buliminella grata*, *Gyroidinoides complanata* and *Stilostomella plummerae*. Less common taxa are *S. gracillima*, *Bulimina semicostata*, *Osangularia mexicana*, *G. naranjoensis*, *Heronallenia pusilla*, *Turrilina brevispira*, *Cibicidoides ungerianus*, *Dentalina* sp.1 and *Coryphostoma* sp.1. This cluster can be subdivided into two subclusters. Species of subcluster A1, such as *G. subglobosa*, *G. complanata*, *G. naranjoensis*, *S. plummerae* and *C. ungerianus*, reach peak relative abundances near the upper part of level δ and in level ε. Taxa from subcluster A2 show large increases in relative abundance in level β, but even more so within level δ. For instance, *N. umbonifera*, a species that occurs at an average relative abundance of ~7%, increases to ~30% within the lower part of level δ. *Osangularia mexicana*, *Dentalina* sp.1 and *Coryphostoma* sp.1 occur almost exclusively at the base of level δ, coeval with the peak relative abundance of *B. grata*.

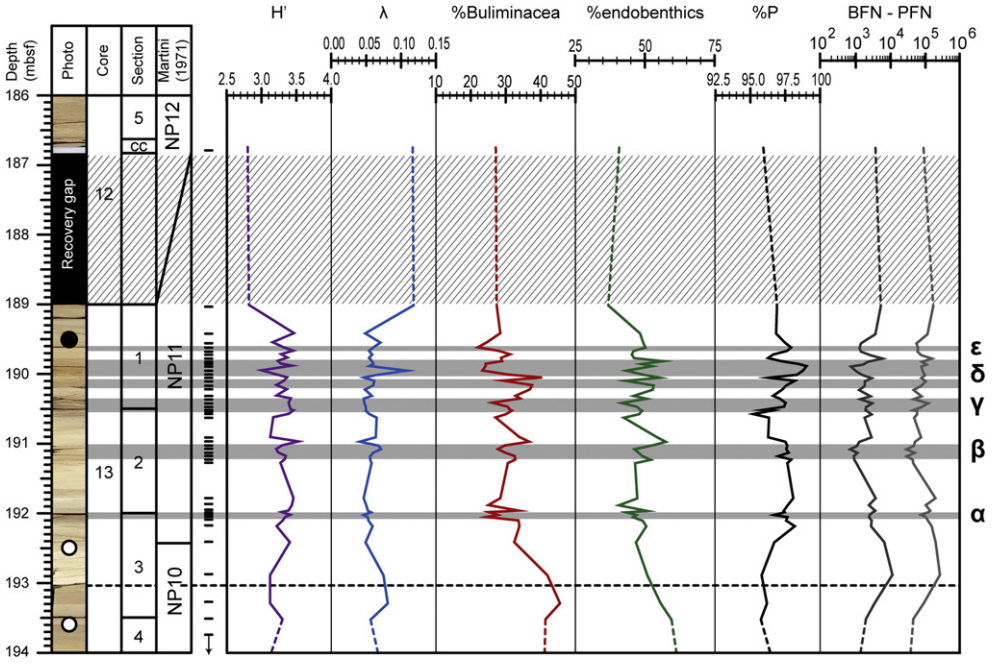

Fig. 3. Benthic foraminiferal assemblage parameters, including diversity (Shannon–Wiener index H′), dominance (λ), relative abundance of Buliminacea, %endobenthic morphotypes, %P, benthic foraminiferal numbers g^{-1} (BFN) and planktic foraminiferal numbers g^{-1} (PFN). Tick marks next to the core photograph represent samples used for the faunal analysis.

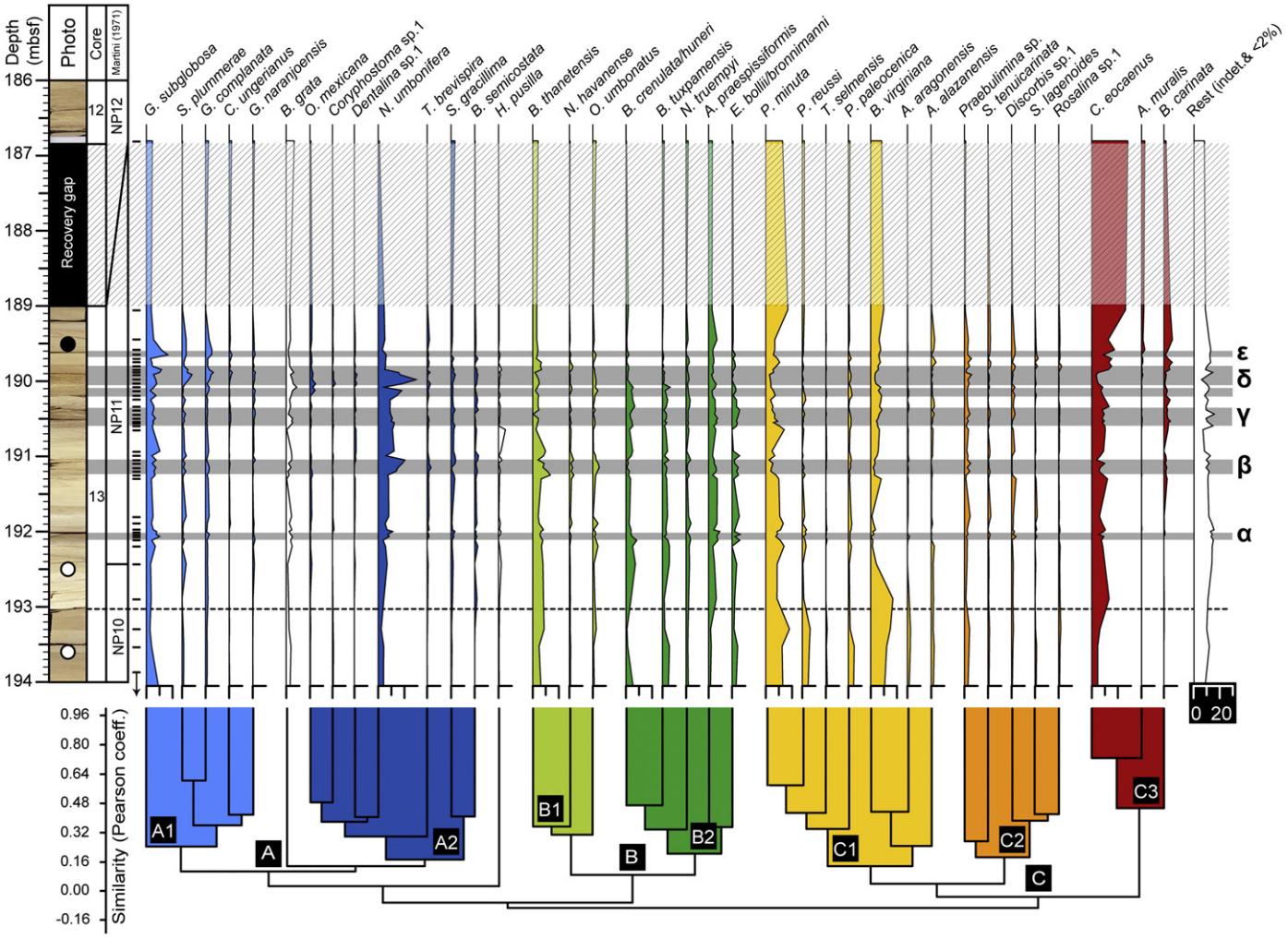

Fig. 4. Relative abundances of the 37 most common taxa (>2%) arranged according to R-mode Cluster Analaysis (CA). Faunal clusters A (A1, A2), B (B1, B2) and C (C1, C2 and C3) are indicated. Tick marks next to the core photograph represent samples used for the faunal analysis.

- Cluster B (*B. thanetensis–A. praespissiformis*): Defined by taxa with relatively stable relative abundance, but that display slight increases in relative abundances within levels α and β. Common taxa include *Bulimina thanetensis*, *Anomalinoides praespissiformis*, *Eponides bollii/bronnimanni*, *Bolivina crenulata/huneri* and *Bulimina tuxpamensis*. Less common taxa include *Oridorsalis umbonatus*, *Nuttallides truempyi* and *Nonion havanense*. This cluster can be subdivided into two subclusters B1 and B2. Taxa from subcluster B1 show little fluctuations within the marly levels, except for level β where there is a slight increase in relative abundance. Taxa from subcluster B2 show little fluctuations within the marly levels, except for the marked relative abundance drop of *B. crenulata/huneri* and *B. tuxpamensis* at the base of level δ.
- Cluster C (*C. eocaenus–P. minuta*): Defined by taxa that occur in high relative abundances in the carbonate-rich intervals and in low relative abundances within the marly levels. Common taxa include *Cibicidoides eocaenus*, *Pseudoparrella minuta*, *Bulimina virginiana*, *Praebulimina* sp.1 and *Brizalina carinata*. Less common taxa are *Pleurostomella paleocenica*, *Discorbis* sp.1, *P. reussi*, *Anomalinoides alazanensis*, *Siphonina tenuicarinata*, *Rosalina* sp.1, *Aragonia aragonensis*, *Seabrookia lagenoides*, *Angulogerina muralis* and *Tappanina selmensis*. This cluster can be subdivided into three subclusters C1, C2 and C3. Taxa from subcluster C1 occur rather consistently across the studied interval, except for the marly levels. This subcluster is characterized by taxa that are particularly abundant in Biozone NP10. Taxa from subcluster C2 show a minor increase in relative abundance above level δ. Taxa from subcluster C3, *C. eocaenus*, *A. muralis* and *B. carinata*, show a gradual increase in relative abundance towards the top of the studied interval but are also characterized by a sudden and significant permanent increase in relative abundance above levels δ and ε.

3.2.2. Definition of foraminiferal biofacies based on detrended correspondence analysis

Based on the first two axes (DCA Axis 1 — detrended Eigenvalue: 0.0828; DCA Axis 2 — detrended Eigenvalue: 0.0537) of the Q-mode DCA — and confirmed by the Q-mode CA — we can distinguish four natural assemblages of organisms, here called biofacies (Figs. 5 and 6; Table 4).

- Biofacies I [194.80–192.90 mbsf]: This biofacies contains all samples of biozone NP10; including the samples below the lithological break. This biofacies is characterized by taxa from all three faunal clusters at more or less equal percentages, but it differs from biofacies II by the larger presence of the endobenthic taxa from cluster C1.
- Biofacies II [192.43–192.25 mbsf]–[192.00–190.19 mbsf]: This biofacies contains samples from the carbonate rich intervals [192.43–190.19 mbsf] and from marly levels α [192.07–192.00 mbsf] and γ

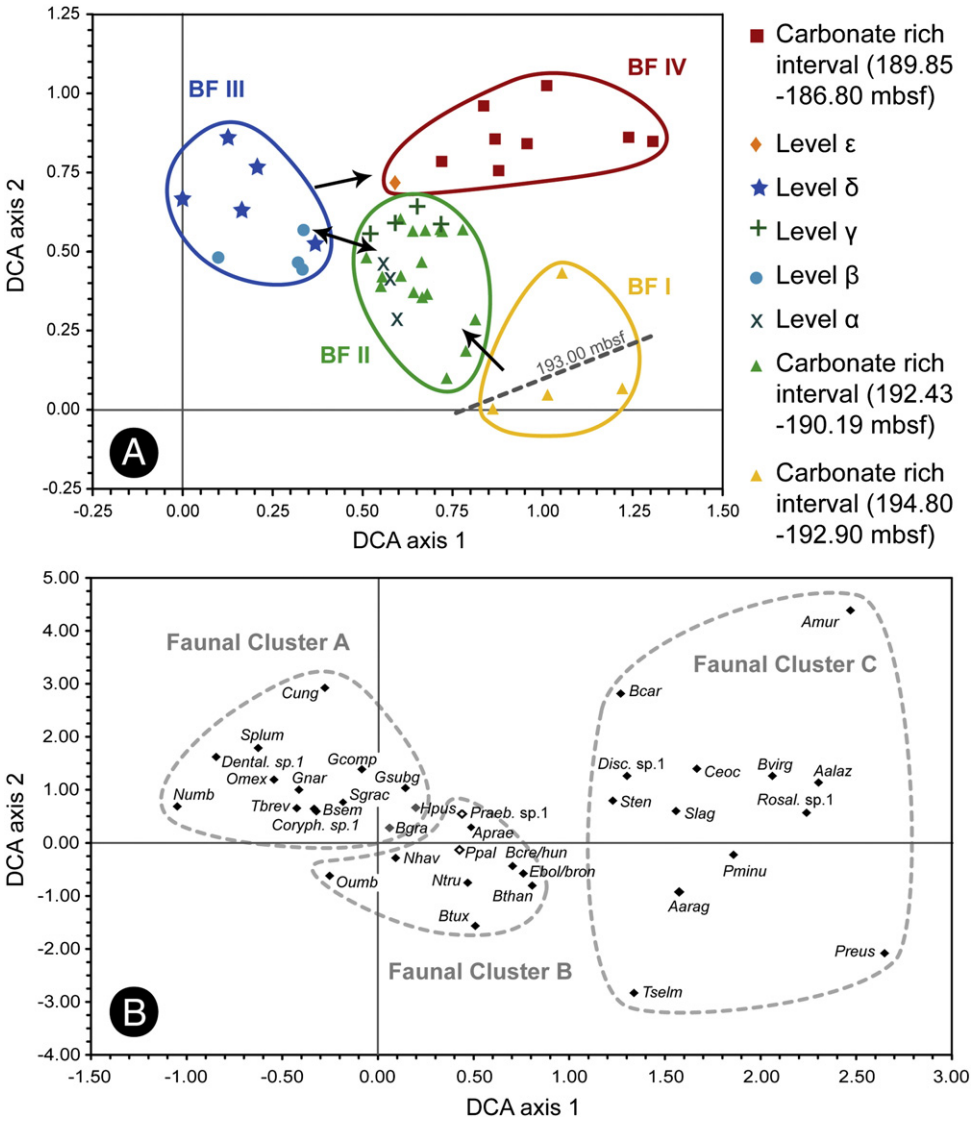

Fig. 5. Results of the Detrended Correspondence Analysis (DCA). (A) Biplot of Q-mode DCA. Circles represent biofacies I to IV. The triangles below the dashed line represent the samples below the lithological break at 193.00 mbsf. Arrows roughly indicate the stratigraphic sequence of the samples. (B) Biplot of R-mode DCA with the 37 most common taxa (>2% rel. abund.). Dashed circles encompass the species representing the three faunal clusters as defined by the Cluster Analysis (CA; see Fig. 4). Hollow diamonds represent species (*Praebulimina* sp.1 and *Pleurostomella paleocenica*) that were placed in faunal cluster C by the CA. Gray diamonds represent species (*Buliminella grata* and *Heronallenia pusilla*) that belong to faunal cluster A, but split off from the main branch early on (Fig. 4).

[190.55–190.44 mbsf]. This biofacies is characterized by taxa from all three faunal clusters at more or less equal percentages.

- Biofacies III [191.20–191.05 mbsf]–[190.13 mbsf]–[190.08–189.89 mbsf]: This biofacies exclusively contains samples of marly levels β and δ. It is dominated by taxa of faunal cluster A (up to 75%). This biofacies is also characterized by the lowest diversity and benthic foraminiferal numbers.
- Biofacies IV [189.85–186.80 mbsf]: This biofacies contains all samples above level δ, including the sample of level ε. This biofacies is dominated by taxa from faunal cluster C and contains only minor amounts of taxa from faunal cluster B.

4. Discussion

4.1. Sedimentology

4.1.1. Sedimentation rates

As a consequence of recovery gaps in cores 12 and 13 (Montadert et al., 1979a) and lithological variations, sedimentation rates cannot be estimated accurately. Using estimates for the duration of the biozones as provided by Berggren et al. (1995), we calculated average sedimentation rates of ~0.5 cm/kyr throughout Biozones NP10–NP12. The observed clear and sharp lithological transition at ~193.00 mbsf likely represents an erosional contact or a non-depositional feature. Across this stratigraphic gap $CaCO_3$ values rise from 70 to 85 wt.%, the number of foraminifera (both planktic and benthic) show a three to four-fold increase, yet the %P remains stable. As a consequence of this gap, the sedimentation rate across the NP10–NP11 boundary cannot be estimated accurately, leaving only an average sedimentation rate for Biozone NP11, which varies between 0.45 and 0.74 cm/kyr depending on the exclusion or inclusion of the recovery gap at the base of core 12 to NP11 — resulting in a maximal sampling resolution of about 5–10 kyr.

As orbital forcing plays a major role in early Paleogene climate and its expression in the geological record (Cramer et al., 2003; Lourens et al., 2005; Westerhold et al., 2007, 2008; Westerhold and Röhl, 2009; Galeotti et al., 2010; Zachos et al., 2010; Sexton et al., 2011), it is not unlikely that the repetitive nature of the marly levels is indeed

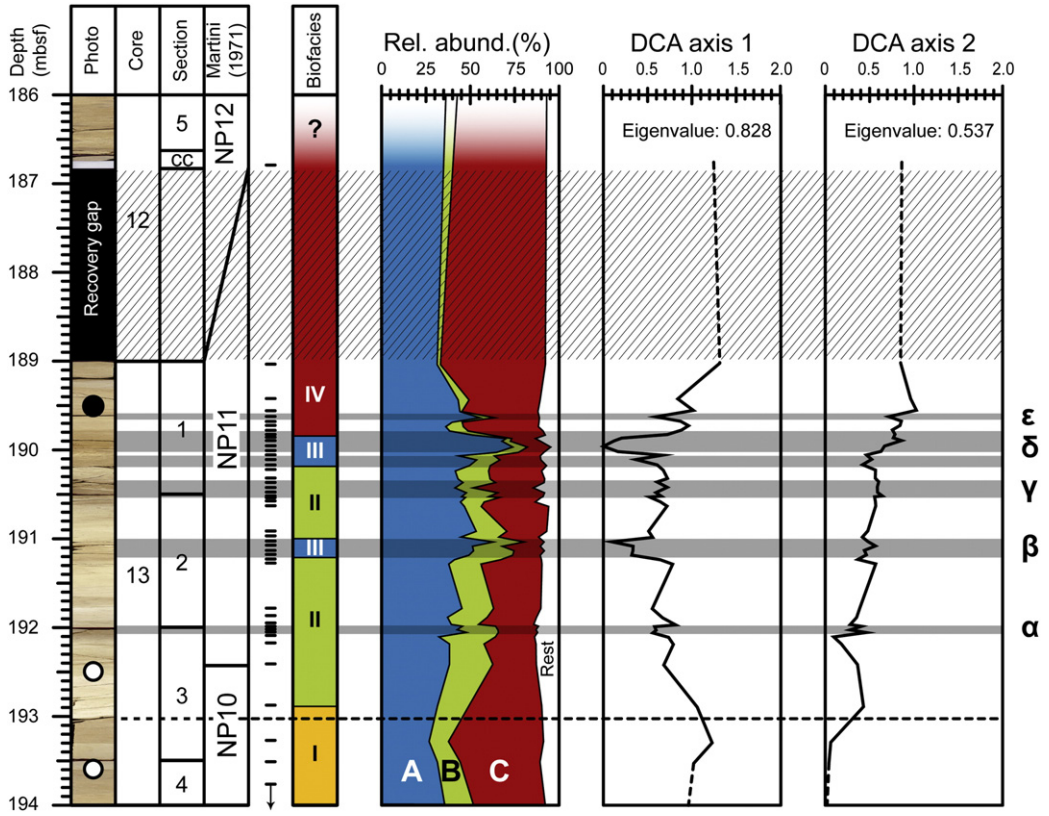

Fig. 6. Foraminiferal biofacies and cumulative relative abundances of the three faunal clusters (A, B and C) plotted versus the 1st and 2nd axes of the Q-mode DCA. Note the transient character of levels β, δ and ε and in particular the near-disappearance of taxa of cluster B and the dominance of taxa of cluster C following levels δ, resulting in biofacies IV. Tick marks represent samples used for the faunal analysis.

the result of Milankovitch cyclicity. Applying the average sedimentation rates for the entire NP11 interval suggests that the marly levels may track the short eccentricity cycle, but as the sedimentation rate is not well constrained across the marly levels, this remains speculative.

4.1.2. $CaCO_3$ content

Although the observed fluctuations in $CaCO_3$ content of the interval (Fig. 2) may be cyclic, it remains unclear what causes them. In deep-sea deposits, $CaCO_3$ content is mainly controlled by one or more of the following factors (Volat et al., 1980):

1) Biogenic $CaCO_3$ production
2) Dilution due to influx of terrigenous material
3) Syn-or postdepositional dissolution

For instance in level δ, the large $CaCO_3$ drop (~80% to ~50%) corresponds to a maximum reduction (dissolution or loss of biogenic $CaCO_3$ production) of the $CaCO_3$ by 75% or a maximum increase in clayey material by 400% or a fitting combination of both. Many deep-sea PETM and early Eocene hyperthermal deposits are associated with dissolution episodes (Zachos et al., 2005; Colosimo et al., 2006; Hancock et al., 2007; Stap et al., 2009; Kelly et al., 2010; Leon-Rodriguez and Dickens, 2010), and thus low $CaCO_3$ content and anomalous coarse fraction percentages due to severe dissolution may be a telltale sign for a hyperthermal. In our material, the lack of dissolution is demonstrated by a very weak negative covariance between $CaCO_3$ content and the amount of coarse fraction ($R^2 = 0.18$). Additionally, we also observed little fragmentation of foraminiferal tests.

Instead, the remarkably high amounts of coarse fraction at the base of level δ (Fig. 2) could reflect ecological factors. Both in recent (Schmidt et al., 2003; Al-Sabouni et al., 2007) and fossil deposits (Kaiho et al., 2006; Petrizzo, 2007) relatively large planktic foraminifera occur in areas with stratified oligotrophic and/or warm surface waters. In our material, the amount of coarse fraction corresponds to the maximum planktic foraminifera size level δ (Fig. 7), suggesting stratified oligotrophic surface waters with possibly diminished

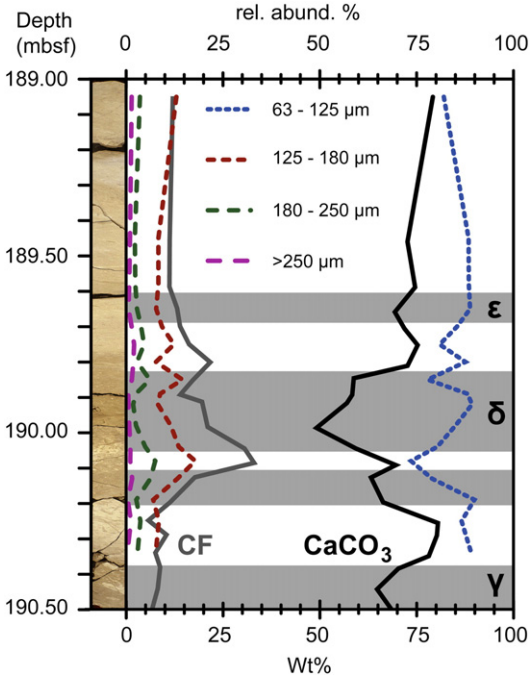

Fig. 7. Planktic foraminiferal test size in the interval 189.05–190.34 mbsf.

biogenic $CaCO_3$ production of calcareous nannoplankton (e.g. Malinverno, et al., 2009). However, the other carbonate-poor marly levels including the core of level δ do not show these high values of CF and larger-sized foraminifera. This implies that another process (e.g. dilution by terrigenous material) played a major role instead. Dilution through the addition of terrigenous material has also been suggested for hyperthermal-related neritic and (hemi)pelagic deposits through the intensification of the hydrological cycle and the resulting increase in continental weathering, terrigenous run-off and/or aeolian dust transport (Bowen et al., 2004; Kelly et al., 2005; Nicolo et al., 2007; Schmitz and Pujalte, 2007; Agnini et al., 2009). Increased dust input may also dilute the $CaCO_3$ accumulation, but it is unlikely to be of such a magnitude to explain the large $CaCO_3$ content variations as observed in our material (e.g. Woodard et al., 2011). It is more likely that large quantities of clay minerals are transported to the deep sea in the form of intermediate or bottom nepheloid layers, as these are important vectors for lateral transport of lithogenic material to the ocean floor (van Weering et al., 1998; McCave et al., 2001). The low-resolution study of Cassat (1979) of Site 401 shows that level δ is characterized by a large increase in kaolinite (~30% of total clay assemblage, with background values of ~10%), a telltale sign for increased continental erosion of the hinterland (Chamley, 1989). Hence, we suggest that, not dissolution, but lateral transport of terrigenous clayey material by intermediate or bottom nepheloid layers is the primary cause for the observed low $CaCO_3$ content in level δ and possibly also in the other marly levels.

4.2. Bulk sediment stable isotopes

The carbon and oxygen isotope record is measured on bulk carbonates and thus represents a complex signature: it contains the signal of the upper part of the water column and a minor component of the sea floor, possibly records early diagenetic effects (Schrag et al., 1995) and differential isotopic signatures of nannoplankton (Ziveri et al., 2003). Therefore, it is not easy to distil clear local, regional or global signals, rendering detailed interpretations speculative. Instead, the stable isotope record on bulk sediments of this study mainly serves a stratigraphic purpose: the observed pattern of negative carbon and oxygen isotope excursions are used to detect and characterize potential hyperthermal-like events and to place them in a timeframe.

The bulk carbonate $\delta^{13}C$ record (Fig. 2) at Site 401 reveals that during NP11, absolute values vary between 0.90 and 1.10‰ for the carbonate-rich intervals. After comparison of this range with records from the NP11–NP12 interval from several DSDP/ODP Sites (550, 577, 690, 762, 1051, 1215, 1262–1267; Thomas et al., 1992; Cramer et al., 2003; Stap et al., 2009; Leon-Rodriguez and Dickens, 2010; Zachos et al., 2010) and land sections from Italy (Contessa, Possagno; Agnini et al., 2009; Galeotti et al., 2010) and New-Zealand (Mead Stream, Dee Stream; Nicolo et al., 2007) we notice that the absolute values are very similar to these sites and land sections and are nearly identical to nearby Northern Hemisphere localities (Sites 550, 1051 and the Contessa road section) (Table 2). When comparing the magnitude

Table 2
Comparison of global stable isotope records on bulk material of biozones NP11–NP12. Values of ranges are absolute, while values noted under α–ε or H1–K are maximum deviations from background values. Note that levels α to ε do not necessarily correspond to global CIEs H1–K. All values are given in ‰ V-PDB. References: 1) Cramer et al., 2003, 2) Galeotti et al., 2010, 3) Agnini et al., 2009, 4) Leon-Rodriguez and Dickens, 2010, 5) Thomas et al., 1992, 6) Zachos et al., 2010, 7) Stap et al., 2009, 8) Röhl et al., 2005, 9) Nicolo et al., 2007.

Site	Site location	Ocean	Paleolatitude	Type	Min. range	Max. range	Δ range	α	β	γ	δ	ε	Reference
401	Meriadzek Terrace	North Atlantic	~43°N	C	0.90	1.10	0.20	0.65	0.29	0.26	0.76	0.39	This study
				O	−0.40	−0.10	0.30	0.57	0.35	0.20	0.59	0.44	

Site	Site location	Ocean	Paleolatitude	Type	Min. range	Max. range	Δ range	Global CIEs H1	H2	I1	I2	K	Reference
550	Goban Spur	North Atlantic	~45°N	C	0.90	1.20	0.30	0.90	0.40	0.68	0.59	0.71	1
				O	−0.80	−0.60	0.20	0.74	0.72	0.60	0.81	0.64	
1051	Blake Nose	North Atlantic	~30°N	C	0.80	1.20	0.40	0.71	0.37	0.62	0.35	–	1
				O	−0.30	0.00	0.30	0.57	0.39	0.49	0.41	–	
–	Contessa	Tethys	~40°N	C	0.95	1.30	0.35	0.63	–	0.39	–	0.57	2
				O	–	–	–	–	–	–	–	–	
–	Possagno	Tethys	~40°N	C	0.70	0.90	0.20	0.30	–	0.30	–	0.20	3
				O	–	–	–	–	–	–	–	–	
577	Shatsky Rise	Equatorial Pacific	~10°N	C	1.30	1.60	0.30	0.77	0.28	0.48	0.18	0.60	1
				O	−0.50	−0.25	0.25	0.30	0.30	0.30	0.30	0.30	
1215	–	Equatorial Pacific	~20°N	C	1.70	1.90	0.20	0.39	–	0.14	–	0.96	4
				O	−1.70	−1.40	0.30	0.13	–	0.27	–	0.83	
690	Maud Rise	South Atlantic	~70°S	C	0.90	1.30	0.40	1.26	–	–	–	–	1
				O	−0.40	−0.10	0.30	0.53	–	–	–	–	
762 C	Exmouth Plateau	South Indian	~45°S	C	1.15	1.25	0.10	–	–	–	–	–	5
				O	−0.90	−0.60	0.30	–	–	–	–	–	
1262	Walvis Ridge	South Atlantic	~35°S	C	1.30	1.65	0.35	0.84	0.58	0.75	0.60	–	6, 7
				O	−0.60	−0.20	0.40	0.70	0.61	0.63	–	–	
1263	Walvis Ridge	South Atlantic	~35°S	C	1.10	1.40	0.30	1.50	0.60	–	–	–	7
				O	−0.55	−0.25	0.30	1.20	0.50	–	–	–	
1265	Walvis Ridge	South Atlantic	~35°S	C	1.15	1.50	0.35	1.00	0.60	–	–	0.60	7, 8
				O	−0.60	−0.30	0.30	0.70	0.50	–	–	0.60	
1267	Walvis Ridge	South Atlantic	~35°S	C	1.20	1.60	0.40	1.00	0.60	–	–	–	7
				O	−0.65	−0.30	0.35	0.70	0.50	–	–	–	
–	Mead/Dee Stream	South Pacific	~50°S	C	1.20	1.50	0.30	0.90	0.20	0.60	0.20	–	9
				O	–	–	–	–	–	–	–	–	
			Northern Hemisphere	C	0.84	1.15	0.31	0.64	0.39	0.50	0.47	0.49	
				O	−0.55	−0.30	0.25	0.66	0.56	0.55	0.61	0.64	
			Equator	C	1.50	1.75	0.25	0.58	0.28	0.31	0.18	0.78	
				O	−1.10	−0.83	0.28	0.22	0.30	0.29	0.30	0.57	
			Southern Hemisphere	C	1.14	1.46	0.31	1.08	0.52	0.68	0.40	0.60	
				O	−0.62	−0.29	0.33	0.77	0.53	0.63	–	0.60	
			Global	C	1.16	1.45	0.29	0.77	0.39	0.49	0.35	0.62	
				O	−0.76	−0.47	0.28	0.55	0.46	0.49	0.46	0.60	

of the CIEs of the marly levels of Site 401 to the magnitude of the global CIEs of Biozone NP11–NP12 (H1 to K; e.g. Cramer et al., 2003), the same relation is observed: the magnitude of the CIEs of levels α and δ is as large as the regional and global average observed for H1 and K — those particular CIEs that are associated with the largest known early Eocene hyperthermals (e.g. Cramer et al., 2003; Stap et al., 2009). Furthermore, the reported magnitude of the CIEs of H1 and K is about half to one third compared to the CIE of the PETM (Lourens et al., 2005; Nicolo et al., 2007; Stap et al., 2009; Galeotti et al., 2010). At Site 401, Pardo et al. (1997) and Nunes and Norris (2006) recorded a CIE for the PETM of ~2.00‰ for *Morozovella subbotinae* and ~1.80‰ for *N. truempyi*. The marly levels in NP11 have bulk CIEs that are about a third or half this magnitude, further suggesting that they may very well represent one or more of these global CIEs.

The bulk carbonate $\delta^{18}O$ record (Fig. 2) largely co-varies with $\delta^{13}C$ ($R^2 = 0.55$), yet during levels γ and δ, a small phase offset exists as $\delta^{18}O$ shifts slightly precede the carbon isotope record and recover more swiftly. Even so, the same general patterns and magnitudes, as seen in the bulk carbonate $\delta^{13}C$ record, emerge. These $\delta^{18}O$ excursions may possibly relate to short-lived rises in (local) temperatures implying a correlation between the CIEs and a rise in (global) temperature, a key feature in all hyperthermals, including the PETM (Lourens et al., 2005; Quillévéré et al., 2008; Sluijs et al., 2009; Leon-Rodriguez and Dickens, 2010; Stap et al., 2010a,b; Zachos et al., 2010).

4.3. Benthic foraminifera

4.3.1. Evaluation of taphonomic effects

In quantitative micropaleontological studies, it is of utmost importance to know whether or not a fossil assemblage mainly represents a primary ecological or a secondary, taphonomic signal (van der Zwaan et al., 1990). Therefore, before providing an ecological interpretation of the assemblages, an assessment of the preservation state of the foraminifera is needed. We observe that the foraminiferal preservation throughout the studied interval is good for larger species (>125 μm) and moderate to good for smaller specimens (>63 μm). Under Reflected Light Microscopy (RLM) most smaller thin-walled species display a slightly more 'milky' or 'frosty' preservation due to minor secondary calcite overgrowths, which was confirmed using Scanning Electron Microscopy (SEM) (Plates 1 and 2). Even so, all specimens revealed features such as sutures, pores and umbilical boss (if present initially) when dry and became completely translucent when wet. Some smooth-walled species (both large and small) such as *G. subglobosa*, *Praebulimina* spp., *Gyroidinoides* spp., *O. umbonatus*, *C. eocaenus*, *B. tuxpamensis* and *N. havanense* showed a shiny (and often translucent) test in all samples when dry. Even though few indications are present for dissolution (i.e. etching of the test wall resulting in an irregular surface, breakage of chambers and the reduction of test size and wall thickness; see Plates 1 and 2) and we previously suggested that dissolution did not play major role (Section 4.1.2), dissolution is a common taphonomic process in the deep-sea and a more thorough assessment is appropriate. So in addition to the preservation state of the (benthic) foraminifera, we also used the following indicators to assess dissolution processes:

(1) %P in combination with foraminiferal numbers and $CaCO_3$ content
(2) Foraminiferal differential dissolution

It is well known that tests of planktic foraminifera are generally more prone to dissolution than those of hyaline benthic foraminifera (e.g. Nguyen et al., 2009). When deep-sea sediments with low $CaCO_3$ content display a low %P and low numbers of foraminifera per gram, it is likely that $CaCO_3$ dissolution has occurred at some step during the generation of the fossil assemblage (van der Zwaan et al., 1990; Speijer and Schmitz, 1998). Overall, %P is >95% at all times and $CaCO_3$ content and %P are barely correlated ($R^2 = 0.15$) suggesting little or no dissolution. The same conclusion can be made for levels δ and ε which – despite their low $CaCO_3$ values – display severe drops in BFN but maximal %P, so dissolution does not seem to have played a role in the formation of the fossil assemblages. On the other hand, levels α and β display small concomitant drops in $CaCO_3$ content, %P and PFN and BFN, possibly suggesting minor dissolution.

Differential dissolution selectively removes susceptible species (mostly thin-walled, small specimens), resulting in an enrichment of the fossil assemblage in more resistant species. This process is known to exist for both planktic taxa as well as benthic taxa (Nguyen et al., 2009). In modern and fossil assemblages, species such as *Gyroidinoides* spp. and *G. subglobosa* have been found to be the most resistant benthic species, while *N. umbonifera*, *O. umbonatus*, *Osangularia* spp. and *Cibicidoides* spp. remain more or less unaffected by dissolution (Corliss and Honjo, 1981; Woodruff and Douglass, 1981; Thomas, 1985; Widmark and Malmgren, 1988). *Praebulimina* spp. is less resistant while Nodosariacea, Buliminacea and *Nonion* spp. are considered the least resistant, and their presence is often used as a marker for the absence of severe dissolution (Corliss and Honjo, 1981; Woodruff and Douglass, 1981; Thomas, 1985; Widmark and Malmgren, 1988; Thomas and Gooday, 1996). Here, differential dissolution does not seem to have affected the assemblages, as dissolution resistant (or susceptible) species' distribution patterns do not covary.

The observed moderate to good preservation of the foraminifera combined with high %P, and the lack of indications of differential dissolution suggest that the observed benthic foraminiferal biofacies shifts mainly represent a reliable primary signal and are not the result of dissolution in the studied interval, including the marly levels.

4.3.2. Ecology of marker species

Jorissen et al. (1995) proposed the conceptual TROX model, connecting the microhabitat characteristics of benthic foraminiferal assemblages to oxygen content and food availability. However, the TROX model is a general model evaluating entire faunal assemblages largely based on endo-epibenthic ratios, but individual taxa may show significant differences in their sensitivity (Fontanier et al., 2002; Jorissen et al., 2007). In this study, we complement this model using often-applied ecological preferences of selected marker species (Table 3) to infer the ecological relevance of each biofacies. However, the ecology of several commonly occurring species such as *P. minuta*, *B. virginiana* and *C. eocaenus* is hitherto not established. Using the CA and DCA (Figs. 4 and 5), their ecology can be inferred by comparison with other better-known species.

The fact that *P. minuta* (frequently reported as *Epistominella minuta*; Boltovskoy, 1983; Poag and Norris, 2005) – and to a lesser extent *B. virginiana* – covary with *T. selmensis* and *A. aragonensis* may imply that these taxa have similar ecological preferences. *Aragonia aragonensis* and *T. selmensis* are frequently found in neritic and bathyal deposits following the PETM (Thomas, 1998, 2003) and other suspected hyperthermal events (Ortiz and Thomas, 2006). They are thought to be opportunistic species associated with (transient) food-rich environments and not necessarily with low oxygen concentrations (Thomas, 1998, 2003). Considering the inferred ecology of *P. minuta* by Poag and Norris (2005), we interpret an increased abundance of *B. virginiana* and *P. minuta* as indications for an increased and episodic (seasonal?) C_{org} supply to the seafloor. We also note that *B. virginiana* has only been found in neritic settings in the Atlantic Coastal Plains of America (Nogan, 1964) and to our knowledge has not been observed in deeper deposits before. As no other typical (outer-) neritic species have been observed continuously in the studied interval, selective suspension and downslope transport of *B. virginiana* specimens seems unlikely. Furthermore, it occurs consistently in large quantities (average of ~5.5%; up to ~17%) and displays virtually no sign of transportation such as abrasion and broken chambers. A possible

Table 3
Summary of the known ecological preferences of selected benthic foraminiferal species.

Angulogerina muralis	Turbiditic environments (~intensified bottom-water or slope currents, high OM flux)	Molina et al., 2006; Ortiz and Thomas, 2006; Ortiz et al., 2008, 2011; Agnini et al., 2009
Aragonia aragonensis	Opportunistic, transient high-food environments	Thomas, 1998, 2003
Bolivinoides crenulata	High input of low-quality OM, high energy environment, opportunistic	Agnini et al., 2009; Ortiz et al., 2011
Bulimina thanetensis	Mesotrophic conditions with (seasonally) fluctuating oxygen and productivity levels	Ernst et al., 2006
Bulimina virginiana	Opportunistic, transient high-food environments	See text
Cibicidoides eocaenus	Enhanced bottom water velocity (?)	See text
Cibicidoides ungerianus	Intolerant for low oxygen levels	den Dulk et al., 1998
Eponides spp.	Well-oxygenated sediments, response to fresh phytodetritus (opportunistic)	Duchemin et al., 2007; Gooday and Rathburn, 1999; Jorissen, 1999
Globocassidulina subglobosa	Oxic conditions	Schönfeld, 2001
	Oligotrophy ($\leq$1 g $Cm^{-2}yr^{-1}$), enhanced bottom water current velocity, located above carbonate corrosive environments	Schmiedl et al., 1997; Mackensen et al., 1995
	Oligotrophy (no seasonal signal)	Sun et al., 2006; Smart, 2008
	Response to seasonal pulse of high-quality, fresh phytodetritus	Miao and Thunell, 1993; Gupta and Thomas, 2003; Gooday, 1988, 1993
	Opportunistic	Alegret et al., 2009, 2010
	Mesotrophic conditions with (seasonally) fluctuating oxygen and productivity levels	Ernst et al., 2006
Gyroidinoides spp.	High oxygen levels/low tolerance for oxygen depletion in bottom and pore waters, oligo-mesotrophy	Schmiedl et al., 2003; Kuhnt et al., 2007; Gupta and Thomas, 2003
	Opportunistic	Gupta and Thomas, 2003; Schmiedl et al., 2003
Nuttallides truempyi	Low-food, tolerant of sluggish circulation	Tjalsma and Lohmann, 1983; Thomas, 1998
	Tolerant of low oxygen concentrations	Widmark and Speijer, 1997
Nuttallides umbonifera	Carbonate corrosive bottom water/restricted to region between lysocline and CCD	Bremer and Lohmann, 1982; Miller, 1983; Mackensen et al., 1990, 1993, 1995; Müller-Merz and Oberhänsli, 1991; Mackensen and Ehrmann, 1992; Harloff and Mackensen, 1997; Schmiedl et al., 1997; Katz et al., 2003
	Oligotrophy (<1.5 g $Cm^{-2}yr^{-1}$)	Loubere, 1991; Schmiedl et al., 1997
	Oligotrophy, no seasonal fluctuations	Sun et al., 2006
	Oxic, well-ventilated bottom waters (*Nuttallides rugosa*)	Kurbjeweit et al., 2000
	Tolerant of sluggish circulation	Miller, 1983
	Low salinities	Mackensen et al., 1995
Oridorsalis umbonatus	Well-oxygenated pore waters, low sustained flux of highly degraded OM	Miao and Thunell, 1993; Mackensen et al., 1995; Gupta and Thomas, 1999, 2003
	No strong relation to high OM fluxes	Mackensen et al., 1995; Schmiedl and Mackensen, 1997
Pseudoparrella minuta	Opportunistic, low oxygen/high food	Poag and Norris, 2005
Stilostomella spp.	Meso-eutrophic, intermediate seasonality of productivity	See text
Tappanina selmensis	Opportunistic, transient high-food environments	Thomas, 1998, 2003

explanation of the lack of reports on this species in deep-sea studies could also be due to its size: its width rarely exceeds 80 μm in our material and consequently, it may have been missed in studies based on larger-sized material. A similar case can be made for the presence of *N. umbonifera*. This species is first commonly observed during the Eocene–Oligocene climate transition (Thomas, 1990, 2007; Mackensen and Ehrmann, 1992; Katz et al., 2003), although it also has been observed as early as the latest Paleocene in the South Atlantic (Thomas, 1990; Thomas and Shackleton, 1996). We suspect that this species is actually a common faunal component in late Paleocene–early Eocene lower bathyal–upper abyssal deposits, at least in the northeast Atlantic Ocean (personal observations), but that because of its small size, it has been underrepresented in previous studies of the Bay of Biscay (e.g. Berggren, 1972; Schnitker, 1979; Miller, 1983; Miller et al., 1985; Pak and Miller, 1992).

In the modern ocean, some species of *Gyroidinoides* (e.g. *G. orbicularis*, *G. neosoldanii* and *G. nitidula*) prefer high oxygen concentrations or they have a low tolerance to oxygen depletion in bottom and pore water (Gupta and Thomas, 2003; Schmiedl et al., 2003; Kuhnt et al., 2007). Furthermore, they are common in oligotrophic environments, although they also occur at higher trophic levels in intermediate to highly seasonal environments, illustrating their opportunistic behavior (Gupta and Thomas, 2003; Schmiedl et al., 2003; Kuhnt et al., 2007). We interpret an increased abundance of *Gyroidinoides* spp. as indicative for oxygenated and oligo–mesotrophic settings with seasonal fluxes of food. The ecology of *Stilostomella* spp. is still widely debated (e.g. Hayward et al., 2010), but in our material, the distribution of *S. plummerae* and *S. gracillima* is relatively similar to *G. complanata* and *G. naranjoensis*, possibly pointing to a somewhat similar paleoecological behavior.

Angulogerina muralis is commonly observed in Eocene turbiditic sections in the Betic Cordillera of southeastern Spain and in sections in the Southern Alps (Molina et al., 2006; Ortiz and Thomas, 2006; Ortiz et al., 2008, 2011; Agnini et al., 2009). In recent sediments Mackensen et al. (1995) and Harloff and Mackensen (1997) found a positive correlation between the presence of *Angulogerina angulosa* and high C_{org} flux rates and coarse grain sizes resulting from strong bottom currents. Bottom-water currents have been shown to influence the microhabitat and composition of the benthic foraminiferal fauna (Mackensen et al., 1995; Schönfeld, 2002a, b). Using this information, we suspect that *A. muralis* is adapted to environments with a high C_{org} flux and intensified bottom water currents.

Cibicidoides eocaenus, which distribution shows the largest similarity with *A. muralis* (Pearson coeff. r = 0.74, Figs. 4 and 5) is a typical epibenthic taxon and occurs mainly in bathyal settings. Its planoconvex morphology suggests an epibenthic mode of life (Jorissen et al., 1999; Fontanier et al., 2002). Cibicidids have regularly been found associated with increased bottom water currents (Schönfeld, 2002a, b; Ortiz et al., 2011), although this relation should be applied cautiously (e.g. Jorissen et al., 2007).

4.4. Paleoenvironmental and paleoceanographic interpretation

4.4.1. Paleodepth and lysocline/CCD depth

Based on the occurrence and abundance of depth-related species and their upper depth limits, we investigated the paleodepth of Site 401. Some species of faunal cluster A form the major constituents of lower Eocene assemblages with an upper depth limit at 1500–1800 m (Miller, 1983; Tjalsma and Lohmann, 1983; Müller-Merz and Oberhänsli, 1991; Katz et al., 2003), while most species from

Table 4
Summary of the four biofacies observed in this study including ecological characteristics and characteristic species.

Biofacies I	Mesotrophy Moderate to high oxygen levels High seasonality of productivity (upwelling/surface water mixing)	*Bulimina virginiana*, *Pseudoparrella minuta*, *Praebulimina reussi*, *Bulimina thanetensis*, *Bulimina tuxpamensis*, *Aragonia aragonensis*, *Tappanina selmensis*
Biofacies II	Oligo-mesotrophy High oxygen levels High seasonality of productivity (upwelling/surface water mixing)	*Pseudoparrella minuta*, *Cibicidoides eocaenus*, *Bulimina thanetensis*, *Anomalinoides praespissiformis*, *Nuttallides umbonifera*, *Bulimina virginiana*, *Bolivina huneri*/*Bolivinoides crenulata*, *Bulimina tuxpamensis*
Biofacies III	Oligotrophy High oxygen levels Limited seasonality of productivity Surface water stratification (?) Increased run-off (?)	*Nuttallides umbonifera*, *Stilostomella* spp., *Globocassidulina subglobosa*, *Gyroidinoides* spp., *Cibicidoides ungerianus*, *Osangularia mexicana*, *Buliminella grata*, *Quadratobuliminella pyramidalis*
Biofacies IV	Oligo-mesotrophy High oxygen levels Moderate seasonality of productivity (upwelling/surface water mixing) Increased bottom water current velocity (?)	*Cibicidoides eocaenus*, *Pseudoparrella minuta*, *Bulimina virginiana*, *Globocassidulina subglobosa*, *Brizalina carinata*, *Bulimina thanetensis*, *Anomalinoides praespissiformis*, *Angulogerina muralis*

faunal cluster C are more characteristic for upper to lower bathyal deposits. These observations suggest a lower bathyal–upper abyssal (~1800–2000 m) depth of deposition for early Eocene sediments at Site 401, which is highly similar to previous estimates based on benthic foraminifera (Schnitker, 1979) – despite the use of different size fractions – and on ostracods (Ducasse and Peypouquet, 1979) and backtracking (Montadert et al., 1979b). Furthermore, the dominance of calcareous taxa and the preservation state of the foraminifera suggest that the Calcite Compensation Depth (CCD) and lysocline were located well below the depositional depth throughout the studied interval, including for the marly levels. This is in line with an inferred depth for the CCD of about 3.5–4 km and for the lysocline of 2.5–3 km depth, for the South Atlantic, Central Equatorial Pacific and the Indian Ocean (Zachos et al., 2005; Colosimo et al., 2006; Zeebe et al., 2009).

4.4.2. Paleoceanographic interpretation

Benthic foraminiferal distribution is mainly based on the availability of food particles and oxygen content of bottom and pore waters (Jorissen et al., 1995), although other factors (e.g. bottom-water temperatures, pH, salinity, sedimentary processes, substrate or biological processes such as competition and predation) may be important as well in specific environments or circumstances (van der Zwaan et al., 1999; Gooday, 2003; Jorissen et al., 2007). Based on sedimentology, the paleoecology of marker species (Table 3) and the relative abundances of taxa, a paleoenvironmental reconstruction can be made for each identified biofacies (Table 4; Fig. 8).

The relatively clay-rich sediments encompassing biofacies I are characterized by *P. minuta*, *B. virginiana*, *A. aragonensis*, *T. selmensis*, and *B. thanetensis* which represent a mesotrophic environment, with episodic, possibly seasonal fluxes of C_{org} and fluctuating, moderate to high oxygen levels. This is also corroborated by the high %endobenthics and high amount of Buliminacea (Fig. 3). The lower foraminiferal numbers and the relatively low $CaCO_3$ content may be indicative for a larger supply of terrigenous (clayey) material and higher sedimentation rates.

Biofacies II, differing from biofacies I by its reduced presence of *A. aragonensis*, *T. selmensis* and *B. virginiana*, but an increased presence *of C. eocaenus*, *B. crenulata*/*huneri*, *A. praespissiformis*, *E. bollii*/*bronnimanni*, *Gyroidinoides* spp., and *N. umbonifera* implies that it is indicative for a well-oxygenated and oligo- to mesotrophic setting that displays a well-developed seasonality of productivity. The

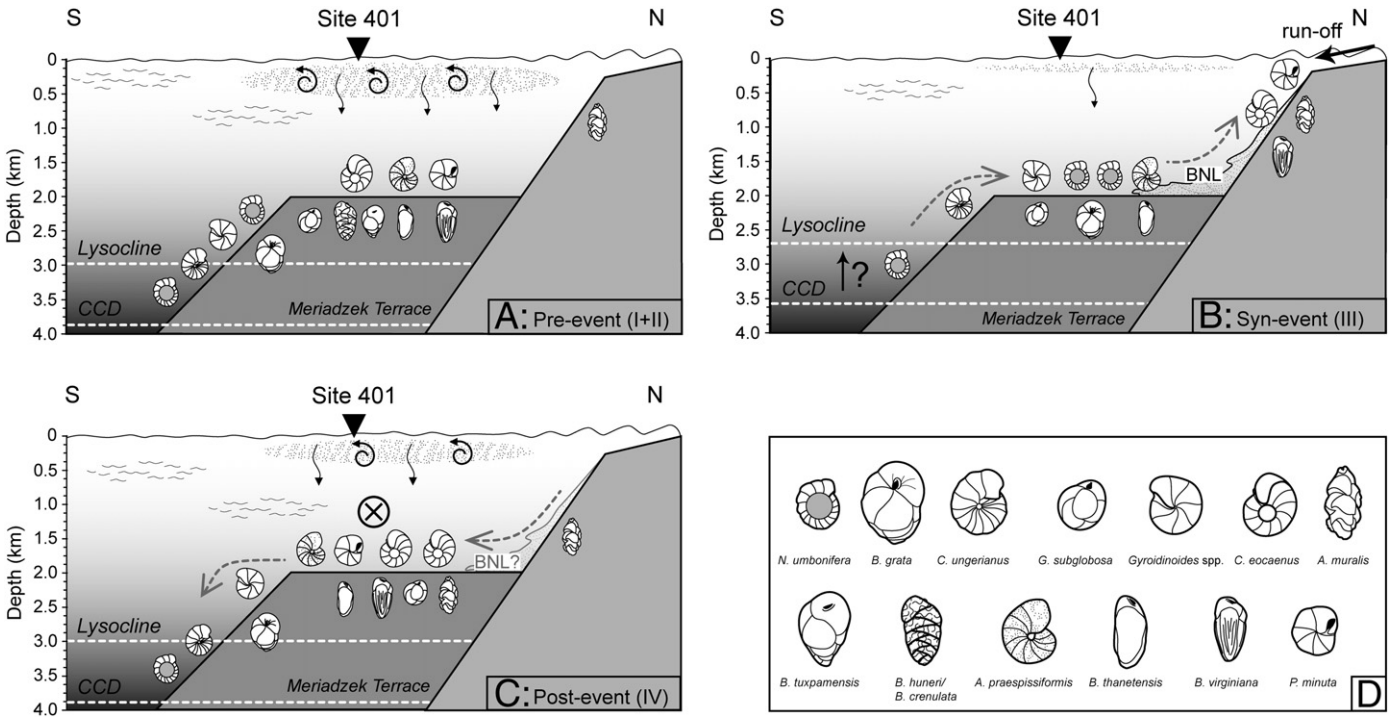

Fig. 8. Postulated paleoceanographic conditions prior, during and after the observed hyperthermal events at DSDP Site 401 at the northern margin of the Bay of Biscay. Dotted area = primary production. Gray arrows = possible migration/repopulation paths of benthic foraminifera. BNL = bottom nepheloid layer. Crossed circle in panel C indicates increased bottom water current activity. (A) Reconstruction prior to the hyperthermal events (Biofacies I and II). (B) Reconstruction during the hyperthermal events (Biofacies III). (C) Reconstruction following the hyperthermal event associated with level δ (Biofacies IV). (D) Schematic representation of selected benthic foraminifera.

lower amount of Buliminacea compared to biofacies I confirms this interpretation (Fig. 3). Overall, the highest $CaCO_3$ values are encountered in samples from this biofacies pointing to a low influx of terrigenous material. Small variations in $CaCO_3$ content are found in levels α and γ, pointing to changes in terrigeneous material influx associated with these levels.

Biofacies III (i.e. marly levels β and δ) is dominated by *N. umbonifera* and is also characterized by a strong decrease of *P. minuta*, *B. virginiana* and *C. eocaenus* while *B. crenulata/huneri* and *B. tuxpamensis* are virtually absent from the record. The common presence of *N. umbonifera* throughout the studied interval and its dominance in biofacies III may indicate that Site 401 was permanently bathed in slightly carbonate corrosive waters, as this species is often found associated with carbonate corrosive bottom waters (see Table 3). However, as stated previously, dissolution does not seem to play an important role in our material. In the present abyssal areas, *N. umbonifera* is not only associated with carbonate corrosive water masses, but its distribution also commonly reflects extremely oligotrophic (Schmiedl et al., 1997) and/or oxygenated bottom waters (Kurbjeweit et al., 2000). Additionally, biofacies III is characterized by the increased presence of *B. grata*, and in sample 189.92 mbsf an isolated occurence of *Quadratobuliminella pyramidalis* (1.6% rel. abund.) is observed. Müller-Merz and Oberhänsli (1991) found that *B. grata* is often associated with *N. truempyi*, suggesting that the large-sized *B. grata* and *Q. pyramidalis* – which is a lower bathyal to abyssal species (Tjalsma and Lohmann, 1983; Van Morkhoven et al., 1986; Katz and Miller, 1996) – are indicators for stable oligotrophic conditions and may be considered as K-selective species. Overall, the dominance of taxa from faunal cluster A during levels β (~60%) and δ (~75%) (Fig. 6) is accompanied by a strong decrease in BFN suggesting that this pattern is mainly the result of a decrease in abundance of taxa from faunal clusters B and C, instead of a bloom of taxa from cluster A. In the present-day Bay of Biscay, a decrease in C_{org} flux is associated with low faunal densities (Fontanier et al., 2002; Mojtahid et al., 2010), so the BFN reflects the oligotrophic nature of levels β and δ. Furthermore, the general loss of opportunistic species may indicate that the oligotrophy is a result of a decline in episodic (seasonal) C_{org} flux. A loss of primary productivity export may be caused by enhanced surface water stratification due to a reduction in upwelling strength or surface water mixing. For level δ, the large size of the planktic foraminifera may indeed be an indication of enhanced stratification although this remains speculative. The low diversity and the significant drop of Buliminacea (in particular level δ) in biofacies III are all additional indications for a stable low-food environment and corroborate this ecological interpretation. Hence, we suggest that biofacies III characterizes well-ventilated oxic and stable oligotrophic conditions with a reduced seasonality of productivity.

The marly levels associated with biofacies III are interpreted as the result of increased erosion of the hinterland and transportation of clayey terrigenous material to the deep sea, Although transportation of sediment particles by nepheloid layers may provide degraded particulate C_{org} to the seafloor (Antia et al., 1999), high temperatures – as suggested by the bulk $\delta^{18}O$ record – may neutralize the effect of this additional food source as increased temperatures enhance metabolic rates (Thomas and Shackleton, 1996; Boersma et al., 1998): the same amount of food may result in a (more) oligotrophic appearing benthic foraminiferal assemblage (Thomas, 2007).

Other species that are also important in biofacies III are *O. umbonatus* and *O. mexicana* and are characteristic for level β and the onset of level δ. *Gyroidinoides* spp., *Stilostomella* spp., *G. subglobosa* and *C. ungerianus* are also characteristic for level β, yet become important in the isotopic recovery of level δ where numbers of *N. umbonifera* are already declining, and indicate well-oxygenated bottom waters and oligotrophic to mesotrophic conditions. The increased presence of the potentially opportunistic *Gyroidinoides* spp. and *G. subglobosa* may imply a reappraisal of seasonality of productivity and organic carbon flux or they may just react opportunistically to a disturbed environment.

Finally, biofacies IV is mainly composed of *C. eocaenus*, *P. minuta*, *B. virginiana*, *G. subglobosa*, *Gyroidinoides* spp. and *B. carinata*. This composition is interpreted as indicative for an oxic and oligo–mesotrophic environment with a well-developed seasonality of productivity as *N. umbonifera* has its lowest relative abundance in this biofacies. Furthermore, the remarkable appearance of *A. muralis*, the strong presence of *G. subglobosa* and *C. eocaenus* in this biofacies may imply an increase in bottom water current velocity at this location, possibly related to an intensification of basin circulation and/or upwelling activity. The doubling of the amount of coarse fraction in this interval compared to the interval containing biofacies II (Fig. 2) might be the result of winnowing, inhibiting the settlement of smaller particles. This apparent intensification of bottom-water currents may have delivered additional refractory C_{org} and may have facilitated small-scale repopulation and migration of lower to middle bathyal species, as indicated by the high BFN and high relative abundances of the abovementioned taxa. The number of Buliminacea remains relatively low for the entire biofacies (with a strong decline in level ε), pointing towards an oxic environment.

The changing trophic patterns across the different biofacies are not observed in the TOC record, which is characterized by extremely low values. C_{org} was probably consumed by the benthic community and/or oxidized, judging by the reddish colored marly levels (Fig. 2). Under such conditions in which TOC values are negligible the benthic foraminifera provide a more powerful and reliable tool to characterize the organic carbon flux to the seafloor (e.g. Jorissen et al., 2007). This illustrates that paleoceanographic conditions cannot and should not be fully constrained from the geochemical record alone and underlines the importance of quantitative micropaleontology.

4.5. Hyperthermal nature?

At DSDP Site 401, the observed negative carbon and oxygen bulk isotope excursions up to ~0.75‰ suggest that injections of ^{12}C-enriched carbon into the ocean–atmosphere system took place, leading to short-term rises in sea-surface temperatures. These isotopic exursions are associated with marly levels amidst a chalky lithology, caused by an increased input of terrigeneous clayey material.

Similar features have been found in all known early Paleogene hyperthermals. Indeed, the main sedimentological and geochemical features are short-lived (<100 kyr) negative excursions ranging between ~0.50‰ to ~1.5‰ (PETM: up to ~4‰) in the bulk, benthic and planktic $\delta^{13}C$ and $\delta^{18}O$ records (Cramer et al., 2003; Lourens et al., 2005; Nicolo et al., 2007; Quillévéré et al., 2008; Agnini et al., 2009; Bornemann et al., 2009; Stap et al., 2009, 2010a,b; Coccioni et al., 2010; Galeotti et al., 2010; Zachos et al., 2010; Sexton et al., 2011; Sprong et al., 2011). Another common feature is the occurrence of carbonate-poor levels, associated with $CaCO_3$ dissolution (Quillévéré et al., 2008; Stap et al., 2009; Coccioni et al., 2010; Leon-Rodriguez and Dickens, 2010) or with dilution due to an increase in terrigenous run-off (Kelly et al., 2005; Nicolo et al., 2007; Agnini et al., 2009). As the marly levels at Site 401 reveal the same characteristics, it is tempting to relate them to hyperthermal events.

On top of the geochemical features, the marly levels of DSDP Site 401 (especially levels β and δ) contain open-marine benthic foraminiferal assemblages that are characterized by the reduction of the diversity, foraminiferal numbers and buliminid species, while oligotrophic benthic foraminiferal species dominate. When combining benthic foraminiferal data of known and suspected hyperthermal events of (hemi-) pelagic settings such as the 'Dan-C2 event' (~65.2 Ma; Coccioni et al., 2010), the 'lower C29n event' (~65.0 Ma; Coccioni et al., 2010), the 'Latest Danian Event' (='top Chron C27n event'; ~61.7 Ma; Speijer, 2003; Bornemann et al., 2009; Sprong et al., 2011; Westerhold et al., 2011), the 'MPBE' (mid-Paleocene biotic event; ~58.2 Ma; Bernaola et al., 2007), the PETM (~55.8 Ma;

Thomas, 1998, 2003, 2007; Takeda and Kaiho, 2007; Alegret et al., 2010), H1 (=ETM2; ~53.7 Ma; Lourens et al., 2005) and K (=ETM3; ~52.5 Ma; Röhl et al., 2005, 2006; Agnini et al., 2009) and the Ypresian–Lutetian boundary event (~48.6 Ma; Ortiz and Thomas, 2006), various overall features emerge. First of all, low diversity/high dominance assemblages characterize all these events indicating stressed conditions at the seafloor. Neritic and hemipelagic settings are mostly characterized by (opportunistic) taxa that are typical for eutrophic and suboxic/anoxic sea-floor conditions such as *T. selmensis*, *A. aragonensis*, *G. subglobosa* and *Neoeponides duwi* (Ernst et al., 2006; Agnini et al., 2009; Alegret et al., 2009; Coccioni et al., 2010; Sprong et al., 2011). Truly open marine settings on the other hand are characterized by taxa that are known for oligotrophic conditions such as *Nuttallides* and abyssaminids (*Q. profunda*, *Abyssamina quadrata* and *A. poagi*) (Pak and Miller, 1992; Thomas and Shackleton, 1996; Thomas, 1998; Lourens et al., 2005; Röhl et al., 2005; Takeda and Kaiho, 2007). Notwithstanding minor local or regional variations (due to differences in latitudinal position, local bathymetry, upwelling activity and/or proximity to the continent), general patterns reveal that during hyperthermals continental margins became more eutrophic and potentially important carbon sinks (Speijer and Wagner, 2002; Gavrilov et al., 2003) while open marine regions became more oligotrophic. It appears that this expansion of the trophic resource continuum (e.g. Hallock, 1987; Hallock et al., 1991; Speijer et al., 1997; Boersma et al., 1998; Thomas, 1998) is also observed at DSDP Site 401.

The faunal changes of DSDP Site 401 display large similarities with various other hyperthermal assemblages and appear to be strongly correlated with the geochemical record, ascertaining our suspicions of the presence of hyperthermals. However, a comparison reveals that DCA 1 is only slightly similar to the $\delta^{13}C$ ($R^2=0.44$) and the $\delta^{18}O$ ($R^2=0.29$) record (Figs. 2 and 6). The reason behind this low correlation is the fact that levels α and γ which display fairly prominent CIEs, do not exhibit any significant faunal change. This observation implies that for Site 401 only levels β, δ – and to a lesser extent level ε – are associated with short-lived paleoceanographic changes involving a change from a (seasonal) mesotrophic environment to a stable oligotrophic one. This implies that the underlying paleoceanographic changes at levels β, δ – and to a lesser degree ε – were sufficiently large and long lasting to invoke a substantial faunal change.

Another striking observation is that the small but apparently permanent faunal composition change across level δ towards biofacies IV lasts at least until the base of Biozone NP12. This signal is also noticeable in the Q-mode CA (Fig. 5) and DCA Axis 2 (Fig. 6). In other words, following level δ, the benthic fauna does not completely return to a pre-level δ composition. This is in contrast with level β where the benthic foraminiferal assemblage recovers swiftly to its pre-event composition. This long-term faunal shift may simply reflect a long-term change in general boundary conditions, independent from the shorter-term changes associated with the CIE. However, this longer-term shift (loss of most buliminids, occurrence of *A. muralis*, dominance of *C. eocaenus* and the increased importance of faunal cluster C relative to A) occurs rapidly across level δ and no similar signals resembling this end member are observed prior to level δ. The strong faunal response combined with the largest geochemical changes are striking and illustrate the exceptional characteristics of level δ, as the other marly levels only show minor faunal compositional changes that are immediatly restored to pre-event conditions.

These considerations lead us to conclude that marly level β and especially level δ are excellent candidates for hyperthermal events while levels α, γ and ε are probably the result of normal background variations given their characteristics. The stratigraphic position of levels β and δ in Biozone NP11 also suggests that one of them may correspond to the globally detected hyperthermal ETM2 (e.g. Cramer et al., 2003; Lourens et al., 2005; Stap et al., 2010a,b), but the lack of an unequivocal bio- and magnetostratigraphic framework for DSDP Site 401 obstructs a clear correlation at this point.

5. Conclusions

1. Five marly intervals (α–ε) characterized by decreased $CaCO_3$ contents and covarying bulk negative carbon and oxygen isotope excursions of up to ~0.75‰ were observed in pelagic sediments of Biozone NP11 (early Eocene). The $CaCO_3$ and stable isotope records at Site 401 strongly suggest that several transient injections of ^{12}C-enriched carbon took place, leading to short-term rises in sea surface temperatures, together with an increased contemporaneous influx of clayey material.
2. Two of these levels (β and δ) display significant benthic foraminiferal perturbations characterized by low diversity, low (benthic) foraminiferal numbers, an increased presence of oligotrophic taxa (e.g. *Nuttallides umbonifera*) and a substantial reduction in the abundance of buliminid taxa (e.g. *Bolivina crenulata*/*huneri* and *Bulimina tuxpamensis*). Level δ further displays a subsequent increase of opportunistic taxa (e.g. *Globocassidulina subglobosa*, *Gyroidinoides* spp.) and a return of mesotrophic bathyal taxa (e.g. *Cibicidoides eocaenus*, *Bulimina virginiana*, *Pseudoparrella minuta* and *Angulogerina muralis*). For these two marly levels there appears to be a correlation between the magnitude of these faunal perturbations and the magnitude of the stable isotope excursions, while the other three marly levels (α, γ and ε) – despite displaying similar isotopic excursions – do not show a significant and clear faunal response. This implies that these marly levels reflect background fluctuations, whereas levels β and δ can be considered as anomalous events.
3. The main underlying causes for these short-lived perturbations in the benthic realm are thought to be a decrease in C_{org} flux to the seafloor (e.g. a decrease of seasonality of surface water productivity resulting in oligotrophy at the seafloor) likely due to decreased upwelling/surface water mixing activity, as suggested by the planktic foraminiferal test size. Additionally, during the deposition of level δ – which is associated with the largest isotope excursion and faunal perturbation – a minor, yet clear and long-lasting shift in benthic foraminiferal composition linked to changing basin circulation (i.e. intensified bottom water currents and/or upwelling activity) occurs.
4. The observed patterns and paleoceanographic interpretations are in line with observations of open-marine settings during early Paleogene hyperthermals, including the PETM, confirming the hyperthermal nature of at least some of these marly levels and supporting the idea that the trophic resource continuum expanded during these events. Our findings suggest that early Eocene hyperthermals and the PETM are expressed in a similar way and are possibly driven by similar processes.

Acknowledgments

This manuscript benefited from very constructive reviews of Gerhard Schmiedl and an anonymous reviewer. We would further like to thank Tanja Kouwenhoven for valuable discussions that helped to improve this manuscript. Michael Joachimski (Universität Erlangen) is thanked for the stable isotope analyses and Manuela Lagrange and Eric Petermann (both Universität Leipzig) for washing samples and analyzing $CaCO_3$ and TOC. This research used samples provided by the Ocean Drilling Program (ODP). ODP is sponsored by the U.S. National Science Foundation (NSF) and participating countries under the management of Joint Oceanographic Institutions (JOI), Inc. Funding for this project was provided by the Research Foundation Flanders (FWO) and the KU Leuven Research Fund to RPS and by the German Research Foundation (DFG) BO 2505/4-1 to AB.

Appendix A. Supplementary data

Supplementary data to this article can be found online at doi:10.1016/j.marmicro.2012.02.006.

References

Agnini, C., Macrì, P., Backman, J., Brinkhuis, H., Fornaciari, E., Giusberti, L., Luciani, V., Rio, D., Sluijs, A., Speranza, F., 2009. An early Eocene carbon cycle perturbation at ~52.5 Ma in the Southern Alps: Chronology and biotic response. Paleoceanography 24, PA2209. doi:10.1029/2008PA001649.

Alegret, L., Thomas, E., 2001. Upper Cretaceous and lower Paleogene benthic foraminifera from northeastern Mexico. Micropaleontology 47 (4), 269–316.

Alegret, L., Thomas, E., 2007. Deep-sea environments across the Cretaceous/Paleogene boundary in the eastern South Atlantic Ocean (ODP Leg 208, Walvis Ridge). Marine Micropaleontology 64 (1–2), 1–17. doi:10.1016/j.marmicro.2006.12.003.

Alegret, L., Thomas, E., 2009. Food supply to the seafloor in the Pacific Ocean after the Cretaceous/Paleogene boundary event. Marine Micropaleontology 73 (1–2), 105–116. doi:10.1016/j.marmicro.2009.07.005.

Alegret, L., Ortiz, S., Molina, E., 2009. Extinction and recovery of benthic foraminifera across the Paleocene–Eocene Thermal Maximum at the Alamedilla section (Southern Spain). Palaeogeography, Palaeoclimatology, Palaeoecology 279 (3–4), 186–200. doi:10.1016/j.palaeo.2009.05.009.

Alegret, L., Ortiz, S., Arenillas, I., Molina, E., 2010. What happens when the ocean is overheated? The foraminiferal response across the Paleocene–Eocene Thermal Maximum at the Alamedilla section (Spain). Geological Society of America Bulletin 122 (9–10), 1616–1624. doi:10.1130/B30055.1.

Al-Sabouni, N., Kucera, M., Schmidt, D.N., 2007. Vertical niche separation control of diversity and size disparity in planktonic foraminifera. Marine Micropaleontology 63, 75–90. doi:10.1016/j.marmicro.2006.11.002.

Antia, A.N., von Bodungen, B., Peinert, R., 1999. Particle flux across the mid-European continental margin. Deep Sea Research Part I 46, 1999–2024.

Berggren, W.A., 1972. Cenozoic biostratigraphy and paleobiogeography of the North Atlantic. In: Laughton, A.S., Berggren, W.A. (Eds.), Initial Reports of the Deep Sea Drilling Project, 12 (14). U.S. Government Printing Office, Washington, pp. 965–1001.

Berggren, W.A., Kent, D.V., Swisher, C.C., Aubry, M.-P., 1995. A revised Cenozoic geochronology and chronostratigraphy. In: Berggren, W.A., Kent, D.V., Swisher, C.C., Aubry, M.-P., Hardenbol, J. (Eds.), Geochronology, Time Scales and Global Stratigraphic Correlation: SEPM Special Publication, 54, pp. 129–212.

Bernaola, G., Baceta, J.I., Orue-Etxebarria, X., Alegret, L., MartÍn-Rubio, M., Arostegui, J., Dinarès-Turell, J., 2007. Evidence of an abrupt environmental disruption during the mid-Paleocene biotic event (Zumaia section, western Pyrenees). Geological Society of America Bulletin 119 (7–8), 785–795. doi:10.1130/B26132.1.

Boersma, A., Premoli Silva, I., Hallock, P., 1998. Trophic models for the well-mixed warm oceans across the Paleocene/Eocene epoch boundary. In: Aubry, M.-P., Lucas, S.G., Berggren, W.A. (Eds.), Late Paleocene–early Eocene Biotic and Climatic Events in the Marine and Terrestrial Records. Columbia University Press, New York, pp. 204–213.

Boltovskoy, E., 1983. Late Cenozoic deep-sea benthic foraminifera off the coast of northwest Africa (DSDP Site 369). Journal of African Earth Sciences 1 (2), 83–102.

Boltovskoy, E., Boltovskoy, D., 1989. Paleocene–Pleistocene benthic foraminiferal evidence of major paleoceanographic events in the eastern South Atlantic (DSDP Site 525, Walvis Ridge). Marine Micropaleontology 14, 283–316.

Boltovskoy, E., Watanabe, S., 1993. Cenozoic monothalamous foraminifers from DSDP Site 525 (southern Atlantic). Marine Micropaleontology 39 (1), 1–27.

Boltovskoy, E., Watanabe, S., 1994. Biostratigraphy of Tertiary and Quaternary benthic bathyal foraminifers of DSDP Site 317 (Tropical Pacific). Marine Micropaleontology 23, 101–120.

Boltovskoy, E., Watanabe, S., Totah, V.I., Vera Ocampo, J., 1992. Cenozoic benthic bathyal foraminifers of DSDP Site 548 (North Atlantic). Marine Micropaleontology 38 (2), 183–207.

Bornemann, A., Schulte, P., Sprong, J., Steurbaut, E., Youssef, M., Speijer, R.P., 2009. Latest Danian carbon isotope anomaly and associated environmental change in the southern Tethys (Nile Basin, Egypt). Journal of the Geological Society of London 166, 1135–1142. doi:10.1144/0016-76492008-104.

Bowen, G.J., Beerling, D.J., Koch, P.L., Zachos, J.C., Quattlebaum, T., 2004. A humid climate state during the Palaeocene/Eocene Thermal Maximum. Nature 432, 495–499. doi:10.1038/nature03115.

Bralower, T.J., 2002. Evidence of surface water oligotrophy during the Paleocene–Eocene Thermal Maximum: nannofossil assemblage data from Ocean Drilling Program Site 690, Maud Rise, Weddell Sea. Paleoceanography 17, 1–9. doi:10.1029/2001PA000662.

Bremer, M.L., Lohmann, G.P., 1982. Evidence for primary control of the distribution of certain Atlantic Ocean benthonic foraminifera by degree of carbonate saturation. Deep Sea Research 29 (8A), 987–998.

Buzas, M.A., Culver, S.J., Jorissen, F.J., 1993. A statistical evaluation of the microhabitats of living (stained) infaunal benthic foraminifera. Marine Micropaleontology 20, 311–320.

Cassat, G., 1979. X-ray mineralogy from Holes 399, 400, 400A, 401, 402 and 402A of Bay of Biscay. In: Montadert, L., Roberts, D.G. (Eds.), Initial Reports of the Deep Sea Drilling Project, 48 (27). U.S. Government Printing Office, Washington, pp. 649–663.

Chamley, H., 1989. Clay Sedimentology. Springer-Verlag, Germany, p. 623.

Clark, M.W., Wright, R.C., 1984. In: Hsü, K.J., LaBrecque, J.L. (Eds.), Paleogene abyssal foraminifers from the Cape and Angola Basins, South Atlantic Ocean. Initial Reports of the Deep Sea Drilling Project, 73 (13). U.S. Government Printing Office, Washington, pp. 459–480.

Coccioni, R., Frontalini, F., Bancalà, G., Fornaciari, E., Jovane, L., Sprovieri, M., 2010. The Dan-C2 hyperthermal event at Gubbio (Italy): global implications, environmental effects, and cause(s). Earth and Planetary Science Letters 297, 298–305. doi:10.1016/j.epsl.2010.06.031.

Colosimo, A.B., Bralower, T.J., Zachos, J.C., 2006. In: Bralower, T.J., Premoli Silva, I., Malone, M.J. (Eds.), Evidence for lysocline shoaling at the Paleocene/Eocene Thermal Maximum on Shatsky Rise, northwest Pacific. Proceedings of the Ocean Drilling Program, Scientific Results, 198 (8). Ocean Drilling Program, College Station TX, pp. 1–36.

Corliss, B.H., Chen, C., 1988. Morphotype patterns of Norwegian Sea deep-sea benthic foraminifera and ecological implications. Geology 16, 716–719.

Corliss, B.C., Honjo, S., 1981. Dissolution of deep-sea benthonic foraminifera. Marine Micropaleontology 27 (4), 356–378.

Cramer, B.S., Wright, J.D., Kent, D.V., Aubry, M.-P., 2003. Orbital climate forcing of $\delta^{13}C$ excursions in the late Paleocene–early Eocene (chrons C24n–C25n). Paleoceanography 18 (4), 1–25. doi:10.1029/2003PA000909.

Crouch, E.M., Heilmann-Clausen, C., Brinkhuis, H., Morgans, H.E.G., Rogers, K.M., Egger, H., Schmitz, B., 2001. Global dinoflagellate event associated with the late Paleocene thermal maximum. Geology 29 (4), 315–318.

Culver, S.J., 2003. Benthic foraminifera across the Cretaceous–Tertiary (K–T) boundary: a review. Marine Micropaleontology 47, 177–226.

den Dulk, M., Reichart, G.J., Memon, G.M., Roelofs, E.M.P., Zachariasse, W.J., van der Zwaan, G.J., 1998. Benthic foraminiferal response to variations in surface water productivity and oxygenation in the northern Arabian Sea. Marine Micropaleontology 35, 43–66.

Dickens, G.R., 2011. Down the rabbit hole: toward appropriate discussion of methane release from gas hydrate systems during the Paleocene–Eocene Thermal Maximum and other past hyperthermal events. Climate of the Past 7 (3), 831–846.

Ducasse, O., Peypouquet, J.P., 1979. In: Montadert, L., Roberts, D.G. (Eds.), Cenozoic ostracodes: their importance for bathymetry, hydrology, and biogeography. Initial Reports of the Deep Sea Drilling Program, 48 (12). U.S. Government Printing Office, Washington, pp. 343–363.

Duchemin, G., Fontanier, C., Jorissen, F.J., Barras, C., Griveaud, C., 2007. Living small-sized (63–150 μm) foraminifera from mid-shelf to mid-slope environments in the Bay of Biscay. Journal of Foraminiferal Research 37 (1), 12–32.

Ernst, S.R., Guasti, E., Dupuis, C., Speijer, R.P., 2006. Environmental perturbation in the southern Tethys across the Paleocene/Eocene boundary (Dababiya, Egypt): foraminiferal and clay mineral records. Marine Micropaleontology 60, 89–111. doi:10.1016/j.marmicro.2006.03.002.

Fontanier, C., Jorissen, F.J., Licari, L., Alexandre, A., Anschutz, P., Carbonel, P., 2002. Live benthic foraminiferal faunas from the Bay of Biscay: faunal density, composition, and microhabitats. Deep Sea Research Part I 49, 751–785.

Galeotti, S., Krishnan, S., Pagani, M., Lanci, L., Gaudio, A., Zachos, J.C., Monechi, S., Morelli, G., Lourens, L., 2010. Orbital chronology of Early Eocene hyperthermals from the Contessa Road section, central Italy. Earth and Planetary Science Letters 290, 192–200. doi:10.1016/j.epsl.2009.12.021.

Gavrilov, Y.O., Shcherbinina, E.A., Oberhänsli, H., 2003. Paleocene–Eocene boundary events in the northeastern Peri-Tethys. In: Wing, S.L., Gingerich, P.D., Schmitz, B., Thomas, E. (Eds.), Causes and Consequences of Globally Warm Climates in the Early Paleogene: Geological Society of America Special Paper, 369, pp. 147–168.

Gibbs, S.J., Bown, P.R., Sessa, J.A., Bralower, T.J., Wilson, P.A., 2006. Nannoplankton extinction and origination across the Paleocene–Eocene Thermal Maximum. Science 314, 1770–1773. doi:10.1126/science.1133902.

Gingerich, P.D., 2006. Environment and evolution through the Paleocene–Eocene Thermal Maximum. Trends in Ecology & Evolution 21 (5), 246–253.

Gooday, A.J., 1988. A response by benthic foraminifera to the deposition of phytodetritus in the deep-sea. Nature 332, 70–73. doi:10.1038/332070a0.

Gooday, A.J., 1993. Deep-sea benthic foraminiferal species which exploit phytodetritus: characteristic features and controls on distribution. Marine Micropaleontology 22, 187–205.

Gooday, A.J., 2003. Benthic foraminifera (Protista) as tools in deep-water paleoceanography: environmental influences on faunal characteristics. Advances in Marine Biology 46, 1–90. doi:10.1016/S0065-2881(03)46002-1.

Gooday, A.J., Rathburn, A.E., 1999. Temporal variability in living deep-sea benthic foraminifera: a review. Earth-Science Reviews 46, 187–212.

Gupta, A.K., Thomas, E., 1999. Latest Miocene–Pleistocene productivity and deep-sea ventilation in the northwestern Indian Ocean (Deep Sea Drilling Project Site 219). Paleoceanography 14 (1), 62–73.

Gupta, A.K., Thomas, E., 2003. Initiation of Northern Hemisphere glaciation and strengthening of the northeast Indian monsoon: Ocean Drilling Program Site 758, eastern equatorial Indian Ocean. Geology 31 (1), 47–50.

Hailwood, E.A., 1979. In: Montadert, L., Roberts, D.G. (Eds.), Paleomagnetism of late Mesozoic to Holocene sediments from the Bay of Biscay and Rockall Plateau, drilled on IPOD Leg 48. : Initial reports of the Deep Sea Drilling Program, 48 (11). U.S. Government Printing Office, Washington, pp. 305–339.

Hallock, P., 1987. Fluctuations in the trophic resource continuum: a factor in global diversity cycles? Paleoceanography 2 (5), 457–471. doi:10.1029/PA002i005p00457.

Hallock, P., Premoli Silva, I., Boersma, A., 1991. Similarities between planktonic and larger foraminiferal evolutionary trends through Paleogene paleoceanographic changes. Palaeogeography, Palaeoclimatology, Palaeoecology 83 (1–3), 49–64. doi:10.1016/0031-0182(91)90075-3.

Hammer, Ø., Harper, D.A.T., 2006. Paleontological Data Analysis. Blackwell Publishing, Oxford, p. 351.
Hammer, Ø., Harper, D.A.T., Ryan, P.D., 2001. PAST: palaeontological statistics software package for education and data analysis. Palaeontologia Electronica 4 (1), 9 http://palaeo-electronica.org/2001_1/past/issue1_01.htm.
Hancock, H.J.L., Dickens, G.R., Thomas, E., Blake, K.L., 2007. Reappraisal of early Paleogene CCD curves: foraminiferal assemblages and stable carbon isotopes across the carbonate facies of Perth Abyssal Plain. International Journal of Earth Sciences 95, 925–946. doi:10.1007/s00531-006-0144-0.
Harloff, J., Mackensen, A., 1997. Recent benthic foraminiferal associations and ecology of the Scotia Sea and Argentine Basin. Marine Micropaleontology 31, 1–29.
Hayward, B.W., Sabaa, A.T., Thomas, E., Kawagata, S., Nomura, R., Schröder-Adams, C., Gupta, A.K., Johnson, K., 2010. Cenozoic record of elongate, cylindrical, deep-sea benthic foraminifera in the Indian Ocean (ODP Sites 722, 738, 744, 758 and 763). Journal of Foraminiferal Research 40 (2), 113–133.
Holbourn, A.E., Henderson, A.S., 2002. Re-illustration and revised taxonomy for selected deep-sea benthic foraminifers. Palaeontologia Electronica 4 (2), 1–36 http://palaeo-electronica.org/paleo/2001_2/foram/issue2_01.htm.
Hulsbos, R.E., 1987. In: van Hinte, J.E., Wise Jr., S.W. (Eds.), Eocene benthic foraminifers from the upper continental rise off New Jersey, Deep Sea Drilling Project Site 605. Initial Reports of the Deep Sea Drilling Project, 93 (10). U.S. Government Printing Office, Washington, pp. 525–538.
Jorissen, F.J., 1999. Benthic foraminiferal successions across Late Quaternary Mediterranean sapropels. Marine Geology 153, 91–101.
Jorissen, F.J., de Stigter, H.C., Widmark, J.G.V., 1995. A conceptual model explaining benthic foraminiferal microhabitats. Marine Micropaleontology 26, 3–15.
Jorissen, F.J., Fontanier, C., Thomas, E., 2007. Paleoceanographical proxies based on deep-sea benthic foraminiferal assemblage characteristics. In: Hillaire-Marcel, C., de Vernal, A. (Eds.), Proxies in Late Cenozoic Paleoceanography (Pt. 2): Biological tracers and biomarkers. Elsevier.
Kaiho, K., Takeda, K., Petrizzo, M.P., Zachos, J.C., 2006. Anomalous shifts in tropical Pacific planktonic and benthic foraminiferal test size during the Paleocene–Eocene Thermal Maximum. Palaeogeography, Palaeoclimatology, Palaeoecology 237, 456–464. doi:10.1016/j.palaeo.2005.12.017.
Katz, M.E., Miller, K.G., 1996. Eocene to Miocene oceanographic and provenance changes in a sequence stratigraphic framework: benthic foraminifers of the New Jersey margin. In: Mountain, G.S., Miller, K.G., Blum, P., Poag, C.W., Twichell, D.C. (Eds.), Proceedings of the Ocean Drilling Program, Scientific Results, 150 (5). Ocean Drilling Program, College Station, TX, pp. 65–95.
Katz, M.E., Tjalsma, R.C., Miller, K.G., 2003. Oligocene bathyal to abyssal benthic foraminifera of the Atlantic Ocean. Micropaleontology 49 (2), 1–45.
Kelly, D.C., Zachos, J.C., Bralower, T.J., Schellenberg, S.A., 2005. Enhanced terrestrial weathering/runoff and surface ocean carbonate production during the recovery stages of the Paleocene–Eocene Thermal Maximum. Paleoceanography 20, 1–11. doi:10.1029/2005PA001163.
Kelly, D.C., Nielsen, T.M.J., McCarren, H.K., Zachos, J.C., Röhl, U., 2010. Spatiotemporal patterns of carbonate sedimentation in the South Atlantic: implications for carbon cycling during the Paleocene–Eocene Thermal Maximum. Palaeogeography, Palaeoclimatology, Palaeoecology 293 (1–2), 30–40. doi:10.1016/j.palaeo.2010.04.027.
Kennett, J.P., Stott, L.D., 1991. Abrupt deep-sea warming, palaeoceanographic changes and benthic extinctions at the end of the Palaeocene. Nature 353, 225–229.
Kuhnt, T., Schmiedl, G., Ehrmann, W., Hamann, Y., Hemleben, C., 2007. Deep-sea ecosystem variability of the Aegean Sea during the past 22 kyr as revealed by benthic foraminifera. Marine Micropaleontology 64, 141–162. doi:10.1016/j.marmicro.2007.04.003.
Kurbjeweit, F., Schmiedl, G., Schiebel, R., Hemleben, C., Pfannkuche, O., Wallmann, K., Schäfer, P., 2000. Distribution, biomass and diversity of benthic foraminifera in relation to sediment geochemistry in the Arabian Sea. Deep Sea Research Part II 47 (14), 2913–2955.
Leon-Rodriguez, L., Dickens, G.R., 2010. Constraints on ocean acidification associated with rapid and massive carbon injections: the early Paleogene record at ocean drilling program site 1215, equatorial Pacific Ocean. Palaeogeography, Palaeoclimatology, Palaeoecology 298 (3–4), 409–420. doi:10.1016/j.palaeo.2010.10.029.
Létolle, R., Vergnaud-Grazzini, C., Pierre, C., 1979. Oxygen and carbon isotopes from bulk carbonates and foraminiferal shells at DSDP Sites 400, 401, 402, 403, and 406. In: Montadert, L., Roberts, D.G., et al. (Eds.), Initial Reports of the Deep Sea Drilling Project, 48 (32). U.S. Government Printing Office, Washington, pp. 741–755.
Loeblich Jr., A.R., Tappan, H., 1988. Foraminiferal Genera and their Classification. Van Nostrand Reinhold, New York. 970 pp., 847 pls.
Loubere, P., 1991. Deep-sea benthic foraminiferal assemblage response to a surface ocean productivity gradient: a test. Paleoceanography 6 (2), 193–204. doi:10.1029/90PA02612.
Lourens, L.J., Sluijs, A., Kroon, D., Zachos, J.C., Thomas, E., Röhl, U., Bowles, J., Raffi, I., 2005. Astronomical pacing of late Palaeocene to early Eocene global warming events. Nature 435, 1083–1087. doi:10.1038/nature03814.
Mackensen, A., Berggren, W.A., 1992. Paleogene benthic foraminifers from the southern Indian Ocean (Kerguelen Plateau): biostratigraphy and paleoecology. In: Wise Jr., S.W., Schlich, R., et al. (Eds.), Proceedings of the Ocean Drilling Program, Scientific Results, 120(34). Ocean Drilling Program, College Station TX, pp. 603–630.
Mackensen, A., Ehrmann, W.U., 1992. Middle Eocene through Early Oligocene climate history and paleoceanography in the Southern Ocean: stable oxygen and carbon isotopes from ODP Sites on Maud Rise and Kerguelen Plateau. Marine Geology 108, 1–27.
Mackensen, A., Grobe, H., Kuhn, G., Fütterer, D.K., 1990. Benthic foraminiferal assemblages from the eastern Weddell Sea between 68 and 73°S: distribution, ecology and fossilization potential. Marine Micropaleontology 16 (3–4), 241–283. doi:10.1016/0377-8398(90)90006-8.
Mackensen, A., Fütterer, D.K., Grobe, H., Schmiedl, G., 1993. Benthic foraminiferal assemblages from the eastern South Atlantic Polar Front region between 35° and 57°S: distribution, ecology and fossilization potential. Marine Micropaleontology 22 (1–2), 33–69.
Mackensen, A., Schmiedl, G., Harloff, J., Giese, M., 1995. Deep-sea foraminifera in the South Atlantic Ocean: ecology and assemblage generation. Micropaleontology 41 (4), 342–358.
Malinverno, E., Triantaphyllou, M.V., Stavrakakis, S., Ziveri, P., Lykousis, V., 2009. Seasonal and spatial variability of coccolithophore export production at the South-Western margin of Crete (Eastern Mediterranean). Marine Micropaleontology 71 (3–4), 131–147. doi:10.1016/j.marmicro.2009.02.002.
Martini, E., 1971. Standard Tertiary and Quaternary calcareous nannoplankton zonation. In: Farinacci, A. (Ed.), Proceedings of the Second Planktonic Conference: Roma, Tecnoscienza, pp. 739–785.
McCave, I.N., Hall, I.R., Antia, A.N., Chou, L., Dehairs, F., Lampitt, R.S., Thomsen, L., van Weering, T.C.E., Wollast, R., 2001. Distribution, composition and flux of particulate material over the European margin at 47°N–50°N. Deep Sea Research Part II 48, 3107–3139.
McInerney, F.A., Wing, S.L., 2011. The Paleocene–Eocene Thermal Maximum: a perturbation of carbon cycle, climate, and biosphere with implications for the future. Annual Review of Earth and Planetary Sciences 39 (1), 489–516. doi:10.1146/annurev-earth-040610-133431.
Miao, Q., Thunell, R.C., 1993. Recent deep-sea benthic foraminiferal distributions in the South China and Sulu Seas. Marine Micropaleontology 22, 1–32.
Miller, K.G., 1983. Eocene–Oligocene paleoceanography of the deep Bay of Biscay: benthic foraminiferal evidence. Marine Micropaleontology 7 (5), 403–440.
Miller, K.G., Katz, M.E., 1987. In: Poag, C.W., Watts, A.B. (Eds.), Eocene benthic foraminiferal biofacies of the New Jersey Transect. Initial Reports of the Deep Sea Drilling Project, 95 (7). U.S. Government Printing Office, Washington, pp. 267–298.
Miller, K.G., Curry, W.B., Ostermann, D.R., 1985. Late Paleogene (Eocene to Oligocene) benthic foraminiferal oceanography of the Goban Spur region, Deep Sea Drilling Project Leg 80. In: de Graciansky, P.C., Poag, C.W., et al. (Eds.), Initial Reports of the Deep Sea Drilling Project, 80 (13). U.S. Government Printing Office, Washington, pp. 505–538.
Mojtahid, M., Griveaud, C., Fontanier, C., Anschutz, P., Jorissen, F.J., 2010. Live benthic foraminiferal faunas along a bathymetrical transect (140–4800 m) in the Bay of Biscay (NE Atlantic). Revue de Micropaleontologie 53, 139–162. doi:10.1016/j.revmic.2010.01.002.
Molina, E., Gonzalvo, C., Ortiz, S., Cruz, L.E., 2006. Foraminiferal turnover across the Eocene–Oligocene transition at Fuente Caldera, southern Spain: no cause–effect relationship between meteorite impacts and extinctions. Marine Micropaleontology 58, 270–286. doi:10.1016/j.marmicro.2005.11.006.
Montadert, L., Roberts, D.G., Auffret, G.A., Bock, W.D., Dupeuble, P.A., Hailwood, E.A., Harrison, W.E., Kagami, H., Lumsden, D.N., Müller, C.M., Schnitker, D., Thompson, R.W., Thompson, T.L., Timofeev, P.P., Bourbon, M., Mann, D., 1979a. In: Montadert, L., Roberts, D.G. (Eds.), Site 401. Initial Reports of the Deep Sea Drilling Program, 48 (4). U.S. Government Printing Office, Washington, pp. 71–123.
Montadert, L., Roberts, D.G., De Charpal, O., Guennoc, P., 1979b. In: Montadert, L., Roberts, D.G. (Eds.), Rifting and subsidence of the northern continental margin of the Bay of Biscay. Initial Reports of the Deep Sea Drilling Project, 48 (54). U.S. Government Printing Office, Washington, pp. 1025–1060.
Müller, C., 1979. In: Montadert, L., Roberts, D.G. (Eds.), Calcareous nannofossils from the North Atlantic (Leg 48). Initial Reports of the Deep Sea Drilling Project, 48 (25). U.S. Government Printing Office, Washington, pp. 589–639.
Müller, G., Gastner, M., 1971. The "Karbonat Bombe", a simple device for the determination of the carbonate content in sediments, soils and other materials. Neues Jahrbuch für Mineralogie Monatshefte 10, 466–469.
Müller-Merz, E., Oberhänsli, H., 1991. Eocene bathyal and abyssal benthic foraminifera from a South Atlantic transect at 20–30°S. Palaeogeography, Palaeoclimatology, Palaeoecology 83, 117–171.
Nguyen, T.M.P., Petrizzo, M.R., Speijer, R.P., 2009. Experimental dissolution of a fossil foraminiferal assemblage (Paleocene–Eocene Thermal Maximum, Dababiya, Egypt): implications for paleoenvironmental reconstructions. Marine Micropaleontology 73, 241–258. doi:10.1016/j.marmicro.2009.10.005.
Nicolo, M.J., Dickens, G.R., Hollis, C.J., Zachos, J.C., 2007. Multiple early Eocene hyperthermals: their sedimentary expression on the New Zealand continental margin and in the deep sea. Geology 35 (8), 699–702. doi:10.1130/G23648A.1.
Nielsen, K.S.S., Nielsen, J.K., Bromley, R.G., 2003. Palaeoecological and ichnological significance of microborings in Quaternary Foraminifera. Palaeontologia Electronica 6 (2), 13 http://palaeo-electronica.org/paleo/2003_1/ichno/issue1_03.htm.
Nogan, D.S., 1964. Foraminifera, stratigraphy, and paleoecology of the Aquia Formation of Maryland and Virginia: Cushman Foundation for Foraminiferal Research, Special Publication, 7. 50 pp.
Nomura, R., 1991. In: Weissel, J., Peirce, J., Taylor, E., Alt, J. (Eds.), Paleoceanography of Upper Maestrichtian to Eocene benthic foraminiferal assemblages at Sites 752, 753, and 754, Eastern Indian Ocean. Proceedings of the Ocean Drilling Program, Scientific Results, 121 (1). Ocean Drilling Program, College Station, TX, pp. 3–29.
Nomura, R., 1995. Paleogene to Neogene deep-sea paleoceanography in the Eastern Indian Ocean: benthic foraminifera from ODP Sites 747, 757 and 758. Micropaleontology 41 (3), 251–290.
Nomura, R., Takata, H., 2005. In: Wilson, P.A., Lyle, M., Firth, J.V. (Eds.), Data report: Paleocene/Eocene benthic foraminifers, ODP Leg 199, Sites 1215, 1220 and 1221, Equatorial central Pacific. Proceedings of the Ocean Drilling Program, Scientific Results, 199 (7). Ocean Drilling Program, College Station, TX, pp. 1–34. doi:10.2973/odp.proc.sr.199.223.2005.

Nunes, F., Norris, R.D., 2006. Abrupt reversal in ocean overturning during the Palaeocene/Eocene warm period. Nature 439, 60–63. doi:10.1038/nature04386.
Ortiz, S., Thomas, E., 2006. Lower–middle Eocene benthic foraminifera from the Fortuna Section (Betic Cordillera, southeastern Spain). Micropaleontology 52 (2), 97–150.
Ortiz, S., Gonzalvo, C., Molina, E., RodrÍguez-Tovar, F.J., Uchman, A., Vandenberghe, N., Zeelmaekers, E., 2008. Palaeoenvironmental turnover across the Ypresian–Lutetian transition at the Agost section, Southeastern Spain: in search of a marker event to define the Stratotype for the base of the Lutetian Stage. Marine Micropaleontology 69 (3–4), 297–313. doi:10.1016/j.marmicro.2008.09.001.
Ortiz, S., Alegret, L., Payros, A., Orue-Etxebarria, X., Apellaniz, E., Molina, E., 2011. Distribution patterns of benthic foraminifera across the Ypresian–Lutetian Gorrondatxe section, Northern Spain: response to sedimentary disturbance. Marine Micropaleontology 78, 1–13. doi:10.1016/j.marmicro.2010.09.004.
Pak, D.K., Miller, K.G., 1992. Paleocene to Eocene benthic foraminiferal isotopes and assemblages: implications for deepwater circulation. Paleoceanography 7 (4), 405–422.
Pardo, A., Keller, G., Molina, E., Canudo, J.I., 1997. Planktic foraminiferal turnover across the Paleocene–Eocene transition at DSDP Site 401, Bay of Biscay, North Atlantic. Marine Micropaleontology 29, 129–158.
Petrizzo, M.R., 2007. The onset of the Paleocene–Eocene Thermal Maximum (PETM) at Sites 1209 and 1210 (Shatsky Rise, Pacific Ocean) as recorded by planktonic foraminifera. Marine Micropaleontology 63, 187–200. doi:10.1016/j.marmicro.2006.11.007.
Poag, C.W., Norris, R.D., 2005. Stratigraphy and paleoenvironments of early postimpact deposits at the USGS-NASA Langley Corehole, Chesapeake Bay Impact Crater. In: Horton, J.W., Powars, D.S., Gohn, G.S. (Eds.), Studies of the Chesapeake Bay Impact Structure — The USGS-NASA Langley Corehole, Hampton, Virginia, and Related Coreholes and Geophysical Surveys, Professional Paper 1688. U.S. Department of the Interior, U.S. Geological Survey.
Proto Decima, F., Bolli, H.M., 1978. In: Bolli, H.M., Ryan, W.B.F. (Eds.), Southeast Atlantic DSDP leg 40 Paleogene benthic foraminifers. Initial Reports of the Deep Sea Drilling Project, 40 (19). U.S. Government Printing Office, Washington, pp. 783–809.
Quillévéré, F., Norris, R.D., Kroon, D., Wilson, P.A., 2008. Transient ocean warming and shifts in carbon reservoirs during the early Danian. Earth and Planetary Science Letters 265, 600–615. doi:10.1016/j.epsl.2007.10.040.
Raffi, I., Backman, J., Pälike, H., 2005. Changes in calcareous nannofossil assemblages across the Paleocene/Eocene transition from the paleo-equatorial Pacific Ocean. Palaeogeography, Palaeoclimatology, Palaeoecology 226, 63–126. doi:10.1016/j.palaeo.2005.05.006.
Raffi, I., Backman, J., Zachos, J.C., Sluijs, A., 2009. The response of calcareous nannofossil assemblages to the Paleocene Eocene Thermal Maximum at the Walvis Ridge in the South Atlantic. Marine Micropaleontology 70 (3–4), 201–212. doi:10.1016/j.marmicro.2008.12.005.
Röhl, U., Westerhold, T., Monechi, S., Thomas, E., Zachos, J.C., Donner, B., 2005. The third and final early Eocene Thermal Maximum: characteristics, timing, and mechanisms of the "X" event. Geological Society of America Abstracts with Program 37 (7), 264.
Röhl, U., Westerhold, T., Monechi, S., Thomas, E., Zachos, J.C., Donner, B., 2006. The third Early Eocene Thermal Maximum: Characteristics, Timing and Mechanisms of the "X" Event. Geophysical Research Abstracts 8, 04560.
Röhl, U., Westerhold, T., Bralower, T.J., Zachos, J.C., 2007. On the duration of the Paleocene–Eocene Thermal Maximum (PETM). Geochemistry, Geophysics, Geosystems 8. doi:10.1029/2007GC001784.
Scheibner, C., Speijer, R.P., 2008. Late Paleocene–early Eocene Tethyan carbonate platform evolution — a response to long- and short-term paleoclimatic change. Earth-Science Reviews 90, 71–102.
Schmidt, D.N., Renaud, S., Bollman, J., 2003. Response of planktic foraminiferal size to late Quaternary climate change. Paleoceanography 18 (2), 1039. doi:10.1029/2002PA000831.
Schmiedl, G., Mackensen, A., 1997. Late Quaternary paleoproductivity and deep water circulation in the eastern South Atlantic Ocean: evidence from benthic foraminifera. Palaeogeography, Palaeoclimatology, Palaeoecology 130, 43–80.
Schmiedl, G., Mackensen, A., Müller, P.J., 1997. Recent benthic foraminifera from the eastern South Atlantic Ocean: dependence on food supply and water masses. Marine Micropaleontology 32, 249–287.
Schmiedl, G., Mitschele, A., Beck, S., Emeis, K.-C., Hemleben, C., Schulz, H., Sperling, M., Weldeab, S., 2003. Benthic foraminiferal record of ecosystem variability in the eastern Mediterranean Sea during times of sapropel S5 and S6 deposition. Palaeogeography, Palaeoclimatology, Palaeoecology 190, 139–164.
Schmitz, B., Pujalte, V., 2007. Abrupt increase in seasonal extreme precipitation at the Paleocene–Eocene boundary. Geological Society of America 35 (3), 215–218. doi:10.1130/G23261A.1.
Schnitker, D., 1979. In: Montadert, L., Roberts, D.G. (Eds.), Cenozoic deep water benthic foraminifers, Bay of Biscay. Initial Reports of the Deep Sea Drilling Project, 48 (15). U.S. Government Printing Office, Washington, pp. 377–413.
Schnitker, D., Tjalsma, L.R.C., 1980. New genera and species of benthic foraminifers from Paleocene and Eocene deep-water deposits. Journal of Foraminiferal Research 10 (3), 235–241.
Schönfeld, J., 2001. Benthic foraminifera and pore-water oxygen profiles: a re-assessment of species boundary conditions at the Western Iberian margin. Journal of Foraminiferal Research 31 (2), 86–107.
Schönfeld, J., 2002a. Recent benthic foraminiferal assemblages in deep high-energy environments from the Gulf of Cadiz (Spain). Marine Micropaleontology 44 (3–4), 141–162. doi:10.1016/S0377-8398(01)00039-1.
Schönfeld, J., 2002b. A new benthic foraminiferal proxy for near-bottom current velocities in the Gulf of Cadiz, northeastern Atlantic Ocean. Deep Sea Research Part I 49 (10), 1853–1875. doi:10.1016/S0967-0637(02)00088-2.
Schrag, D.P., DePaolo, D.J., Richter, F.M., 1995. Reconstructing past sea surface temperatures: correcting for diagenesis of bulk marine carbonate. Geochimica et Cosmochimica Acta 59 (11), 2265–2278.
Schröder, C.J., Scott, D.B., Medioli, F.S., 1987. Can smaller benthic foraminifera be ignored in paleoenvironmental analyses? Journal of Foraminiferal Research 17 (2), 101–105.
Sexton, P.F., Norris, R.D., Wilson, P.A., Pälike, H., Westerhold, T., Röhl, U., Bolton, C.T., Gibbs, S., 2011. Eocene global warming events driven by ventilation of oceanic dissolved organic carbon. Nature 471, 349–353. doi:10.1038/nature09826.
Sluijs, A., Röhl, U., Schouten, S., Brumsack, H.-J., Sangiorgi, F., Sinninghe Damsté, J.S., Brinkhuis, H., 2008. Arctic late Paleocene–early Eocene paleoenvironments with special emphasis on the Paleocene–Eocene Thermal Maximum (Lomonosov Ridge, Integrated Ocean Drilling Program Expedition 302). Paleoceanography 23 (1), 1–17. doi:10.1029/2007PA001495 (PA1S11).
Sluijs, A., Schouten, S., Donders, T.H., Schoon, P.L., Röhl, U., Reichart, G.-J., Sangiorgi, F., Kim, J.-H., Sinninghe Damsté, J.S., Brinkhuis, H., 2009. Warm and wet conditions in the Arctic region during Eocene Thermal Maximum 2. Nature Geoscience 2, 777–780. doi:10.1038/NGEO668.
Smart, C.W., 2008. Abyssal NE Atlantic benthic foraminifera during the last 15 kyr: relation to variations in seasonality of productivity. Marine Micropaleontology 69, 193–211. doi:10.1016/j.marmicro.2008.07.007.
Speijer, R.P., 2003. Danian–Selandian sea-level change and biotic excursion on the southern Tethyan margin (Egypt). In: Wing, S.L., Gingerich, P.D., Schmitz, B., Thomas, E. (Eds.), Causes and Consequences of Globally Warm Climates in the Early Paleogene: Geological Society of America, Special Papers, 369, pp. 275–290.
Speijer, R.P., Schmitz, B., 1998. A benthic foraminiferal record of Paleocene sea level and trophic/redox conditions at Gebel Aweina, Egypt. Palaeogeography, Palaeoclimatology, Palaeoecology 137, 79–101. doi:10.1016/S0031-0182(97)00107-7.
Speijer, R.P., Wagner, T., 2002. Sea-level changes and black shales associated with the late Paleocene Thermal Maximum: organic–geochemical and micropaleontologic evidence from the southern Tethyan margin (Egypt–Israel). In: Koeberl, C., Macleod, K.G. (Eds.), Catastrophic Events and Mass Extinctions: Impacts and Beyond: Boulder Colorado: Geological Society of America Special Paper, 356, pp. 533–549.
Speijer, R.P., Schmitz, B., van der Zwaan, G.J., 1997. Benthic foraminiferal extinction and repopulation in response to latest Paleocene Tethyan anoxia. Geology 25 (8), 683–686.
Sprong, J., Youssef, M.A., Bornemann, A., Schulte, P., Steurbaut, E., Stassen, P., Kouwenhoven, T.J., Speijer, R.P., 2011. A multi-proxy record of the Latest Danian Event at Gebel Qreiya, Eastern Desert, Egypt. Journal of Micropaleontology 30, 167–182.
Stap, L., Sluijs, A., Thomas, E., Lourens, L.J., 2009. Patterns and magnitude of deep sea carbonate dissolution during Eocene Thermal Maximum 2 and H2, Walvis Ridge, southeastern Atlantic Ocean. Paleoceanography 24, PA1211. doi:10.1029/2008PA001655.
Stap, L., Lourens, L.J., Thomas, E., Sluijs, A., Bohaty, S., Zachos, J.C., 2010a. High-resolution deep-sea carbon and oxygen isotope records of Eocene Thermal Maximum 2 and H2. Geology 38, 607–610. doi:10.1130/G30777.1.
Stap, L., Lourens, L., van Dijk, A., Schouten, S., Thomas, E., 2010b. Coherent pattern and timing of the carbon isotope excursions and warming during Eocene Thermal Maximum 2 as recorded in planktic and benthic foraminifera. Geochemistry, Geophysics, Geosystems 11, Q11011.
Sun, X., Corliss, B.H., Brown, C.W., Shower, W.J., 2006. The effect of primary productivity and seasonality on the distribution of deep-sea benthic foraminifera in the North Atlantic. Deep Sea Research Part I 53, 28–47. doi:10.1016/j.dsr.2005.07.003.
Sztrákos, K., 2005. Paleocene and lowest Eocene foraminifera from the North Pyrenean trough (Aquitaine, France). Revue de Micropaleontologie 48, 175–236. doi:10.1016/j.revmic.2005.06.001.
Takeda, K., Kaiho, K., 2007. Faunal turnovers in central Pacific benthic foraminifera during the Paleocene–Eocene Thermal Maximum. Palaeogeography, Palaeoclimatology, Palaeoecology 251, 175–197. doi:10.1016/j.palaeo.2007.02.026.
Thomas, E., 1985. In: Mayer, L., Theyer, F. (Eds.), Late Eocene to recent deep-sea benthic foraminifers the Central Equatorial Pacific Ocean. Initial Reports of the Deep Sea Drilling Project, 85 (17). U.S. Government Printing Office, Washington, pp. 655–694.
Thomas, E., 1990. In: Barker, P.F., Kennett, J.P. (Eds.), Late Cretaceous through Neogene deep-sea benthic foraminifers (Maud Rise, Weddell Sea, Antarctica). Proceedings of the Ocean Drilling Program, Scientific Results, 113 (35). Ocean Drilling Program, College Station, TX, pp. 571–594.
Thomas, E., 1998. Biogeography of the late Paleocene benthic foraminiferal extinction. In: Aubry, M.-P., Lucas, S.G., Berggren, W.A. (Eds.), Late Paleocene–Early Eocene Biotic and Climatic Events in the Marine and Terrestrial Records. Columbia University Press, New York, pp. 214–243.
Thomas, E., 2003. Extinction and food at the seafloor: a high-resolution benthic foraminiferal record across the Initial Eocene Thermal Maximum, Southern Ocean Site 690. In: Wing, S.L., Gingerich, P.D., Schmitz, B., Thomas, E. (Eds.), Causes and Consequences of Globally Warm Climates in the Early Paleogene: Boulder Colorado: Geological Society of America Special Paper, 369, pp. 319–332.
Thomas, E., 2007. Cenozoic mass extinctions: what perturbs the largest habitat on Earth? In: Monechi, S., Coccioni, R., Rampino, M.R. (Eds.), Large Ecosystem Perturbations: Causes and Consequences: Geological Society of America Special Paper, 424, pp. 1–23. doi:10.1130/2007.2424(01).
Thomas, E., Gooday, A.J., 1996. Cenozoic deep-sea benthic foraminifers; tracers for changes in oceanic productivity? Geology 24 (4), 355–358.
Thomas, E., Shackleton, N.J., 1996. The Paleocene–Eocene benthic foraminiferal extinction and stable isotope anomalies. In: Knox, R.W.O'b., Corfield, R.M., Dunay, R.E. (Eds.), Correlation of the Early Paleogene in Northwest Europe: Geological Society London Special Publication, 101, pp. 401–441.

Thomas, E., Zachos, J., 2000. Was the late Paleocene Thermal Maximum a unique event? Geologiska Foereningens i Stockholm Foerhandlingar 122, 169–170.
Thomas, E., Shackleton, N.J., Hall, M.A., 1992. In: von rad, U., Haq, B.U. (Eds.), Data report: Carbon isotope stratigraphy of Paleogene bulk sediments, Hole 762C (Exmouth Plateau, Eastern Indian Ocean). Proceedings of the Ocean Drilling Program, Scientific Results, 122(56). Ocean Drilling Program, College Station, TX, pp. 897–901.
Tjalsma, L.R.C., 1983. In: Barker, P.F., Carlson, R.L., Johnson, D.A. (Eds.), Eocene to Miocene benthic foraminifers from Deep Sea Drilling Project Site 516, Rio Grande Rise, South Atlantic. Initial Reports of the Deep Sea Drilling Project, 72 (33). U.S. Government Printing Office, Washington, pp. 731–755.
Tjalsma, R.C., Lohmann, G.P., 1983. Paleocene–Eocene bathyal and abyssal benthic foraminifera from the Atlantic Ocean. Micropaleontology Special Publications 4, 1–90.
Tripati, A.K., Elderfield, H., 2005. Deep-sea temperature and circulation changes at the Paleocene–Eocene Thermal Maximum. Science 308, 1894–1898. doi:10.1126/science.1109202.
van der Zwaan, G.J., Jorissen, F.J., de Stigter, H.C., 1990. The depth dependency of planktonic/benthic foraminiferal ratios: constraints and applications. Marine Geology 95, 1–16.
van der Zwaan, G.J., Duijnstee, I.A.P., den Dulk, M., Ernst, S.R., Jannink, N.T., Kouwenhoven, T.J., 1999. Benthic foraminifers: proxies or problems? A review of paleoecological concepts. Earth-Science Reviews 46, 213–236.
Van Morkhoven, F.P.C.M., Berggren, W.A., Edwards, A.S., 1986. Cenozoic cosmopolitan deep-water benthic foraminifera. Bulletin des Centres de Recherches Exploration-Production Elf- Aquitaine, Memoire 11 421 pp.
van Weering, T.C.E., Hall, I.R., de Stigter, H.C., McCave, I.N., Thomsen, L., 1998. Recent sediments, sediment accumulation and carbon burial at Goban Spur, NW European Continental Margin (47–50°N). Progress in Oceanography 42, 5–35. doi:10.1016/S0079-6611 (98)00026-3.
Volat, J.-L., Pastouret, L., Vergnaud-Grazzini, C., 1980. Dissolution and carbonate fluctuations in Pleistocene deep-sea cores: a review. Marine Geology 34 (1–2), 1–28. doi:10.1016/0025-3227(80)90138-3.
Wachter, E., Hayes, J.M., 1985. Exchange of oxygen isotopes in carbon dioxide–phosphoric acid systems. Chemical Geology 52 (3–4), 365–374. doi:10.1016/0168-9622(85)90046-6.
Westerhold, T., Röhl, U., 2009. High resolution cyclostratigraphy of the early Eocene — new insights into the origin of the Cenozoic cooling trend. Climate of the Past 5, 309–327 www.clim-past.net/5/309/2009/.
Westerhold, T., Röhl, U., Laskar, J., Raffi, I., Bowles, J., Lourens, L.J., Zachos, J.C., 2007. On the duration of magnetochrons C24r and C25n and the timing of early Eocene global warming events: implications from the Ocean Drilling Program Leg 208 Walvis Ridge depth transect. Paleoceanography 22, PA2201. doi:10.1029/2006PA001322.
Westerhold, T., Röhl, U., Raffi, I., Fornaciari, E., Monechi, S., Reale, V., Bowles, J., Evans, H.F., 2008. Astronomical calibration of the Paleocene time. Palaeogeography, Palaeoclimatology, Palaeoecology 257, 377–403. doi:10.1016/j.palaeo.2007.09.016.
Westerhold, T., Röhl, U., Donner, B., McCarren, H.K., Zachos, J.C., 2011. A complete high-resolution Paleocene benthic stable isotope record for the central Pacific (ODP Site 1209). Paleoceanography 26, PA2216. doi:10.1029/2010PA002092.
Widmark, J.G.V., Malmgren, B.J., 1988. Differential dissolution of upper Cretaceous deep-sea benthonic foraminifers from the Angola basin, South Atlantic Ocean. Marine Micropaleontology 13, 47–78.
Widmark, J.G.V., Speijer, R.P., 1997. Benthic foraminiferal ecomarker species of the terminal Cretaceous (late Maastrichtian) deep-sea Tethys. Marine Micropaleontology 31, 135–155.
Wing, S.L., Harrington, G.J., Smith, F.A., Bloch, J.I., Boyer, D.M., Freeman, K.H., 2005. Transient floral change and rapid global warming at the Paleocene–Eocene boundary. Science 310, 993–996. doi:10.1126/science.1116913.
Woodard, S.C., Thomas, D.J., Hovan, S., Röhl, U., Westerhold, T., 2011. Evidence for orbital forcing of dust accumulation during the early Paleogene greenhouse. Geochemistry, Geophysics, Geosystems 12 (2). doi:10.1029/2010GC003394.
Woodruff, F., Douglas, R.C., 1981. Response of deep-sea benthic foraminifera to Miocene paleoclimatic events, DSDP Site 289. Marine Micropaleontology 6, 617–632.
Zachos, J.C., Wara, M.W., Bohaty, S.M., Delany, M.L., 2003. A transient rise in tropical sea surface temperature during the Paleocene–Eocene Thermal Maximum. Science 302, 1551–1554. doi:10.1126/science.1090110.
Zachos, J.C., Röhl, U., Schellenberg, S.A., Sluijs, A., Hodell, D.A., Kelly, D.C., Thomas, E., Nicolo, M., Raffi, I., Lourens, L.J., McCarren, H., Kroon, D., 2005. Rapid acidification of the ocean during the Paleocene–Eocene Thermal Maximum. Science 308, 1611–1615. doi:10.1126/science.1109004.
Zachos, J.C., McCarren, H., Murphy, B., Röhl, U., Westerhold, T., 2010. Tempo and scale of late Paleocene and early Eocene carbon isotope cycles: implications for the origin of hyperthermals. Earth and Planetary Science Letters 299, 242–249. doi:10.1016/j.epsl.2010.09.004.
Zeebe, R., Zachos, J.C., 2007. Reversed deep-sea carbonate ion basin gradient during Paleocene–Eocene Thermal Maximum. Paleoceanography 22, PA3201. doi:10.1029/2006PA001395.
Zeebe, R.E., Zachos, J.C., Dickens, G.R., 2009. Carbon dioxide forcing alone insufficient to explain Palaeocene–Eocene Thermal Maximum warming. Nature Geoscience 2, 576–580. doi:10.1038/NGEO578.
Ziveri, P., Stoll, H., Probert, I., Klaas, C., Geisen, M., Ganssen, G., Young, J., 2003. Stable isotope 'vital effects' in coccolith calcite. Earth and Planetary Science Letters 210 (1–2), 137–149. doi:10.1016/S0012-821X(03)00101-8.